Journal of Cleaner Production 427 (2023) 139081

Contents lists available at ScienceDirect

Journal of Cleaner Production

journal homepage: www.elsevier.com/locate/jclepro

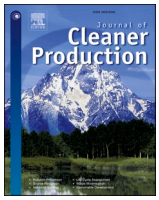

Toward green steel: Modeling and environmental economic analysis of iron direct reduction with different reducing gases

Antonio Trinca [a,*], Daniele Patrizi [a], Nicola Verdone [a], Claudia Bassano [b], Giorgio Vilardi [a]

[a] "Sapienza" University of Rome, Dept. of Chemical Engineering Materials Environment, Via Eudossiana 18, 00184, Rome, Italy
[b] ENEA - Italian Agency for New Technologies, Energy and Sustainable Economic Development, Via Anguillarese 301, 00123, Rome, Italy

ARTICLE INFO

Handling Editor: Giovanni Baiocchi

Keywords:
Decarbonization
Hydrogen
Electrolysis
MSW gasification
Process simulation
Carbon capture

ABSTRACT

The objective of the paper is to simulate the whole steelmaking process cycle based on Direct Reduced Iron and Electric Arc Furnace technologies, by modeling for the first time the reduction furnace based on kinetic approach, to be used as a basis for the environmental and techno-economic plant analysis by adopting different reducing gases. In addition, the impact of carbon capture section is discussed. A complete profitability analysis has been conducted for the first time, adopting a Monte Carlo simulation approach.

In detail, the use of syngas from methane reforming, syngas and hydrogen from gasification of municipal solid waste, and green hydrogen from water electrolysis are analyzed. The results show that the Direct Reduced Iron process with methane can reduce CO_2 emissions by more than half compared to the blast furnace based-cycle, and with the adoption of carbon capture, greenhouse gas emissions can be reduced by an additional 40%. The use of carbon capture by amine scrubbing has a limited economic disadvantage compared to the scenario without it, becoming profitable once carbon tax is included in the analysis. However, it is with the use of green hydrogen from electrolyzer that greenhouse gas emissions can be cut down almost completely. To have an environmental benefit compared with the methane-based Direct Reduced Iron process, the green hydrogen plant must operate for at least 5136 h per year (64.2% of the plant's annual operating hours) on renewable energy.

In addition, the use of syngas and separated hydrogen from municipal solid waste gasification is evaluated, demonstrating its possible use with no negative effects on the quality of produced steel. The results show that hydrogen use from waste gasification is more economic with respect to green hydrogen from electrolysis, but from the environmental viewpoint the latter results the best alternative. Comparing the use of hydrogen and syngas from waste gasification, it can be stated that the use of the former reducing gas results preferable, from both the economic and environmental viewpoint.

1. Introduction

Steel is a critical material in the modern world and its industry is a fundamental sector in terms of both commercial and emissions perspectives. In 2020, global crude steel production reached 1.88 billion tons (Gt) and was responsible for emitting 2.21 Gt of CO_2, according to the World Steel Association (Basson Edwin), (Energy Agency, 2021). Steel production predominantly relies on two methods: blast furnace-basic oxygen furnace (BF-BOF) (73.2% share in EU) and electric arc furnace (EAF) (26.3% share in EU), which account for 99.5% of the total production. The remaining 0.5% of steel is produced from open hearth and other technologies (Suer et al., 2022). BF-BOF technology uses coke as a reducing agent and to produce heat (C and CO), essential in turning iron ore into steel (Deng and Adams, 2020). Iron and steelmaking are among the most energy-intensive processes globally and contribute to 7–9% of global CO_2 emissions, while accounting for 8% of the global energy demand (Impact of Hydrogen DRI on EAF Steelmaking - Midrex)– (Ernst et al., 2023). The conventional BF-BOF manufacturing process traditionally requires 500 kg of coal/t steel, emitting approximately 1.9 t of CO_2 per ton of liquid steel (Mandova et al., 2018), (Cavaliere, 2019). Compared to the integrated BF-BOF route, EAF production is inherently low-carbon. Research indicates that the carbon footprint per ton of EAF steel can vary from 0.23 to 0.46 tCO_2, depending on the iron source (pig iron or scrap), electricity sources, and efficiencies. This would be only 10–20% of conventional BF-BOF operations (Kirschen et al., 2011a).

* Corresponding author.
E-mail address: antonio.trinca@uniroma1.it (A. Trinca).

https://doi.org/10.1016/j.jclepro.2023.139081
Received 11 July 2023; Received in revised form 16 September 2023; Accepted 27 September 2023
Available online 9 October 2023

EAF's ability to play a more significant role in decarbonizing the steelmaking industry is hindered by several limitations. Firstly, since EAF relies on recycled steel scraps as feedstocks, it is susceptible to supply limitations. Furthermore, to effectively have a carbon footprint reduction, the electrical power supply should be from renewable energy sources.

A good solution to increase the output of the EAF and make up for the scrap shortage is Direct Reduced Iron (DRI) technology (Nduagu et al., 2022). At present, the DRI-EAF process covers about 5% of world steel production (Gielen et al.). Direct Reduced Iron production is a solid-state process that operates at temperatures lower than the melting point of iron requiring reduced temperatures for its direct reduction reaction. Reducing gas, which is commonly a mixture of hydrogen and carbon monoxide CO, is usually produced from natural gas or coal. The reduction by CO, remains the main source of CO_2 emissions. Currently, the DRI-EAF route that utilizes natural gas (NG) has a carbon footprint that is only 62% of the traditional integrated BF-BOF route (Longbottom et al., 2008). MIDREX direct reduction technology and Hojalata y Lámina (HYL) Energiron are the leading direct reduction processes because of their high-performance parameters, both in terms of efficiency and productivity (Jiang et al., 2013). They are the most competitive methods for obtaining high-quality DRI for steel production. In detail, MIDREX route contributes 65% of global DRI production (Ranzani Da Costa et al., 2013).

Several studies have attempted to model the DRI-EAF production route with methane.

Parisi and Laborde (2004) simulated the shaft furnace reactor of the MIDREX process. The iron ore reduction kinetics was modeled with the unreacted shrinking core model. The model was able to satisfactorily reproduce the data of two MIDREX plants: Siderca (Argentina) and Gilmore Steel Corporation (U.S.A.). Always based on Gilmore plant data, Shams and Moazeni (2015) simulated and modeled the Midrex shaft furnace, using the model to study the effect of reactor length and cooling gas flow on the metallization and the effect of cooling gas flow on the outlet temperature of the solid phase. Sarkar et al. developed a thermodynamic Model for MIDREX Reduction Shaft. The model was extended to hydrogen rich alternative fuels namely Coke Oven Gas (COG) and Syngas from coal gasification to predict emissions and energy for producing crude steel.

Additionally, DRI production has the potential for deeper decarbonization since the reduction gas can be readily substituted with higher H_2 mixtures or even pure hydrogen (Neuwirth et al., 2021), (Dhawan et al., 2022). In contrast, BF-BOF encounters greater challenges with increased H_2 utilization due to retrofitting barriers (Longbottom et al., 2008), (Yilmaz et al., 2017).

Ranzani Da Costa et al. (2013) developed after experimental and modeling studies, a 2D, axisymmetrical steady-state model called REDUCTOR to simulate a counter-current moving bed reactor in which hematite pellets are reduced by pure hydrogen. Hoxha et al. (2020) detailed a DRI process adapted to use a feed of pure H_2 produced by electrolysis with renewable energy.

However, according to the authors, there is a lack of a validated model in the literature that is able to describe the entire DRI process, including eventual CO_2 capture units, and that can serve as a basis for evaluating alternatives to natural gas for reducing greenhouse gas (GHG) emissions. Modeling of the plant scale has been rarely conducted in comparison to the shaft furnace; just two authors investigated the relationship between the reformer and the shaft furnace, employing mathematical models for each individual unit with kinetic approach (Bechara et al., 2018), (Alhumaizi et al., 2012). This study aims to model the entire process, and not just the individual reduction furnace, by implementing reduction kinetics. The developed model is validated on the basis of data from the Gilmore plant. After validation, the inclusion of a carbon capture and storage (CCS) unit is evaluated. CCS is a viable solution for reducing emissions while waiting for green technologies to become technically and economically applicable on an industrial scale (Lee et al., 2022). Next, the coupling of the production process with an electrolysis unit for using pure hydrogen and a municipal solid waste (MSW) gasification process is proposed. Hydrogen is considered a pivotal solution in the efforts to reduce carbon emissions in steel production. It is seen as a key element in transitioning the industry towards more sustainable and environmentally friendly practices. The findings suggest that the global steel industry will experience a substantial increase in demand for green hydrogen, projected to range from 2809 to 4371 TWh_{H2} by 2050 (Lopez et al., 2022). However, considering the high energy cost of producing green hydrogen, it is also useful to consider other green sources of reducing gas. Waste-source syngas is seen as a hopeful substitute for fossil energy and reductants presently utilized in ironmaking. This is owing to its renewable nature, advanced technological development, and suitability for integration into existing furnaces (Nurdiawati et al., 2023). The current study evaluates the effects of utilizing syngas and hydrogen derived from MSW gasification in the production of direct reduced iron.

The five plant schemes, i.e. natural gas (DRI-NG) and natural gas with carbon capture and storage (DRI-NG-CCS) cases, hydrogen case from electrolyzer (DRI-H_2), syngas case from MSW gasification (DRI-Syngas MSW), and hydrogen case from MSW gasification (DRI-H_2 MSW) are also analyzed from an economic and environmental point of view.

The developed model is intended to be a valuable contribution to research on the decarbonization of the steel industry. Specifically, it has been validated using plant data and possesses the versatility to accommodate various reducing gases from diverse sources. This enables a comprehensive comparison of different production methods, allowing for a thorough evaluation of the economic, energy, and environmental aspects across the entire production cycle.

2. Process layout

2.1. Reaction kinetics

Reduction reactions from hematite to iron take place inside the reduction furnace at temperature above 570 °C.

Reduction by hydrogen is globally endothermic while by CO is globally exothermic (Patisson et al., 2021).

The presence of a certain amount of carbon in DRI is recommended, as it offers several advantages in EAF steel production; these advantages include lowering the melting point of metallic iron, foaming of slag, avoidance of sticking and reoxidation, reduction of electricity demand and thus improvement of the life of EAF refractories and electrodes (Sandeep Kumar et al.). Carburization occurs by means of methane and CO and allows the formation of cementite, with the benefits already listed, according to the following reactions (Table 1). In addition, the presence of methane, CO and water in the furnace at high temperatures leads to the steam methane reforming (SMR) and water gas shift reactions (WGS) occurring.

Table 1 reports kinetic for all the reaction that occur in the shaft furnace with their reference.

2.2. Data validation

The literature data to be used as a comparison for model validation of a DRI plant are very few. The most comprehensive data are those reported for the Gilmore Steel Corporation Plant (Midrex technology) in Portland, Oregon, U.S.A. Several studies report Gilmore data (Table 2) (Parisi and Laborde, 2004), (Shams and Moazeni, 2015), (Hosseinzadeh et al., 2022).

Fig. 1 shows the size of the shaft furnace at the Gilmore plant. The shaft is 9.75 m high and has a diameter of 4.26 m.

The unit is designed to produce 26.4 t of DRI. Other plant data will be discussed in the results chapter, where they will be compared with the results of the DRI-NG model for the validation of the simulation.

Table 1
Reactions and relatively kinetics. S_h is the specific surface areas per mol for hematite (239 m^2/mol). C_h, C_m, C_w are the hematite, magnetite and wustite molar concentration, respectively.

	Reaction	Rate (kmol/(m^3■s))	K	E_a (kJ/mol)	K_{eq}
H_2 Reduction (Hou et al., 2012)	$3Fe_2O_3 + H_2 \leftrightarrow 2Fe_3O_4 + H_2O$	$kC_hS_he^{-\frac{Ea}{RT}}$	4.6×10^4 (m/s)	105.37	–
	$Fe_3O_4 + H_2 \leftrightarrow 3FeO + H_2O$	$kC_mS_he^{-\frac{Ea}{RT}}\left(C_{H_2} - \frac{C_{H2O}}{K_m}\right)$	1.3×10^5 (m/s)	131.46	$76.22 \times 10^4 e^{-\frac{10^3}{RT}}$
	$FeO + H_2 \leftrightarrow Fe + H_2O$	$kC_wS_he^{-\frac{Ea}{RT}}\left(C_{H_2} - \frac{C_{H2O}}{K_w}\right)$	9.5 (m/s)	75.95	$2.01 \times e^{-\frac{511.4}{RT}}$
CO Reduction (Mondal et al., 2004)	$Fe_2O_3 + 2CO \leftrightarrow 2FeO + 2CO_2$	$ke^{-\frac{Ea}{RT}}\left(C_{CO} - \frac{C_{CO2}}{K_{eq}}\right)$	0.08 (s^{-1})	9.97	$1,231.96 \times e^{-\frac{475.22}{RT}}$
	$FeO + CO \leftrightarrow Fe + CO_2$	$ke^{-\frac{Ea}{RT}}\left(C_{CO} - \frac{C_{CO2}}{K_{eq}}\right)$	0.124 (s^{-1})	14.13	$10^{-3} \times e^{-\frac{516.15}{RT}}$
CO Carburization (Mondal et al., 2004)	$3Fe + 2CO \leftrightarrow Fe_3C + CO_2$	$ke^{-\frac{Ea}{RT}}\left(C_{CO} - \frac{C_{CO2}}{K_{eq}}\right)$	10^{-3} (s^{-1})	14.65	$10^{-14} \times e^{-\frac{29726}{RT}}$
CH_4 Carburization (Nasiri et al., 2016)	$3Fe + CH_4 \leftrightarrow Fe_3C + 2H_2$	$ke^{-\frac{Ea}{RT}}\left(C_{CH4} - \frac{C_{H2}}{K_{eq}}\right)$	0.77 (s^{-1})	0.64	$10^{-14} \times e^{-\frac{5447.50}{RT}}$
SMR (Smith Lewin et al., 2020)	$CH_4 + H_2O \leftrightarrow CO + 3H_2$	$ke^{-\frac{Ea}{RT}}\left(P_{CH4}P_{H2O} - \frac{P_{CO}P_{H2}^3}{K_{g4}}\right)$	7.3×10^{-2} (s^{-1})	36.15	$log_{10}\,K = \frac{41837}{T_g} - 0.03$
WGS (Smith Lewin et al., 2020)	$CO + H_2O \leftrightarrow CO_2 + H_2$	$ke^{-\frac{Ea}{RT}}\left(C_{CO}C_{H2O} - \frac{C_{CO2}C_{H2}}{K_{eq}}\right)$	2.78 (s^{-1})	12.6	$0.03 \times 10^4 e^{-\frac{32970}{RT}}$

Table 2
Operating conditions of Gilmore Midrex Plant (Parisi and Laborde, 2004), (Shams and Moazeni, 2015), (Hosseinzadeh et al., 2022).

Feed Gas	
Flow rate (Nm^3/h)	53,863
Temperature (°C)	930
Pressure (barg)	1.4
Feed Gas Composition (%)	
H_2	52.58
CO	29.97
H_2O	4.65
CO_2	4.80
$CH_4 + N_2$	8.1
Solid	
Production (t/h)	26.4
Inlet Temperature (°C)	35
Feed Solid Composition (%)	
Fe_2O_3	95
Gangue	5

Table 3
Syngas from MSW gasification composition (Salman and Omer, 2020).

Syngas Composition (%)	
CH_4	negligible
H_2	49.7
CO	41.4
CO_2	8.9

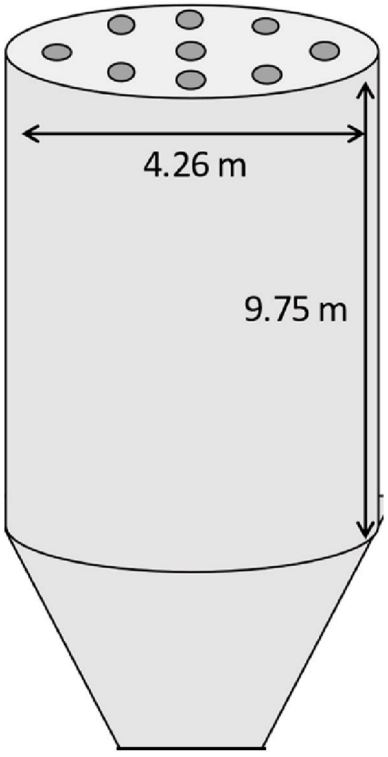

Fig. 1. Gilmore shaft furnace.

2.3. Modeling tool

The simulations are conducted utilizing version V12.1 of the Aspen Plus software. Aspen Plus, software developed by the company Aspen-Tech, is the market-leading chemical process simulator (or at least in the world of chemical engineering). The software allows the user to build a process model and then simulate it using complex calculations (models, equations, mathematical calculations, regressions, etc.). It enables the rigorous calculation of material and energy flows within a process, ensuring mass and energy conservation throughout the system.

The tear flow convergence parameters and the default convergence method were implemented in the Aspen environment, according to the following criteria.

- Tolerance: 10^{-4}
- Tears:Wegstein
- Single Design Spec:Secant
- Multiple Design Spec: Broyden
- Tears and Design Spec:Broyden
- Optimization:SQP

The reactions are implemented using the Langmuir-Hinshelwood-Hougen-Watson (LHHW) model so that the reaction is forward and backward. The LHHW kinetics offer a highly effective and rational

methodology for representing reaction data by considering the involvement of surface concentrations of reactant species in the reaction process (Aslam et al., 2016).

The results of Aspen simulations are collected and reprocessed using excel sheets for energy and environmental analysis. Economic analyses are conducted on excel and using the latest version of Capcost (Capcost_2017. xlsm). Capcost is a Microsoft Excel macro-enabled file that allows the calculation of Equipment Costs, Total Plant Cost, Cost of Manufacturing (COMd), cash flow analysis, and Monte Carlo simulations of cash flows. The program was developed for use with the textbook Analysis, Synthesis and Design of Chemical Processes, fifth edition, by Turton, Shaeiwitz, Bhattacharyya, and Whiting and available from Prentice Hall Publishing.

2.4. DRI-NG model

The published data of the Gilmore plant concerns the furnace dimensions and the flow rates and temperatures of the solid and gaseous input to the furnace. No data is reported for the rest of the plant. The plant diagram is therefore developed based on Midrex's specifications. Choices are also made to minimize the consumption of methane and energy.

Fig. 2 shows the flowsheet developed on Aspen Plus to model the plant (see Fig. 3).

In a typical Midrex plant, the reducing gas used for iron ore reduction is syngas from methane reforming. The calculation is initialized using the flow rate and compositions reported for the Gilmore plant, published in the literature.

The reactor is sized to produce 26.4 t/h.

The shaft furnace is surrounded by several main units including the reformer, scrubber, and heat exchangers. Starting from the gas outlet of the well furnace, the scrubber is the first step, in which part of the water vapor is separated from the rest of the stream. The Aspen unit adopted is a separator, in which the fraction of H_2O separated is defined, in order to optimize the amount of water to be sent to the reforming step. After the top gas is scrubbed downstream from the furnace, it is split into two streams. The first stream is mixed with natural gas and directed towards the reformer's catalytic tubes to produce the reducing gas. The second stream, along with some additional natural gas, is combusted with air to generate heat for the reformer. The Midrex reformer is a "dry" reformer in which the primary reactions are:

$$CH_4 + CO_2 \leftrightarrow 2CO + 2H_2$$

$$CH_4 + H_2O \leftrightarrow CO + 3H_2$$

For a better understanding of how the Midrex process works, the authors recommend reading the following source (Cavaliere, 2019).

In the corresponding Aspen Plus model, after exiting the shaft furnace top gas, the first step is the scrubber, which separates a small portion of the water vapor from the stream. The remaining off-gas is then divided into two streams: one goes to the reformer, and the other goes to the burner. The division at the splitter is done in such a way as to have a flow rate at the shaft inlet equal to that of the Gilmore plant. The stream going to the reformer is mixed with fresh methane, which is controlled to achieve the desired metallization of the DRI. The input current to the reformer has a temperature of 580 °C, consistent with Midrex's proposals for optimization (Midrexa). The built-in Aspen Plus "Gibbs reactor" is used to model the reformer, which does not consider kinetics but calculates the product composition by minimizing its Gibbs energy at equilibrium. This simplification is commonly used in the modeling process (Ye et al., 2009), (Jensen and Duyar, 2021). The reactor works at 900 °C and 2.7 bars (Midrexb), (Sloop). Before being sent back to the shaft furnace, the gas stream exiting the reformer is combined with combustion gas from a burner (Gibbs reactor, adiabatic mode), which involves injecting oxygen and fresh methane, and performing combustion. Oxygen is provided by an air separation unit (ASU), not simulated here. This solution is adopted for additional energy input and temperature control at the furnace inlet (Bechara et al., 2018), (Atsushi et al.). The reducing gas comes in the shaft at 1.4 bar g, according to plant data.

The remaining off-gas from the shaft, methane, and combustion air are the input streams of the combustion system. These streams are preheated and burned, generating hot flue gases that are cooled before being discharged. The burner is modeled as a Gibbs reactor operating at 1 bar and in adiabatic mode. The burner's purpose is to supply energy to the reforming system. This process is then followed by cooling the flue gas to recover energy, which can be used for pre-heating purposes.

The shaft furnace is the core of the process. It is modeled using two

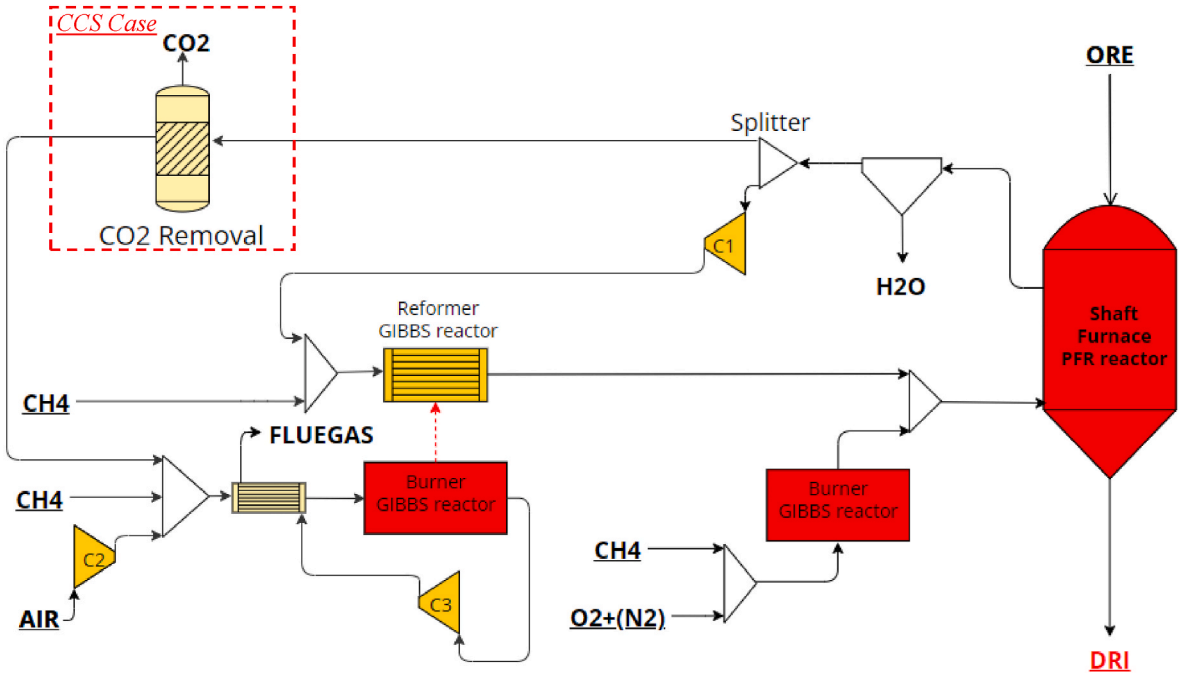

Fig. 2. DRI-NG and DRI-NG-CCS scheme.

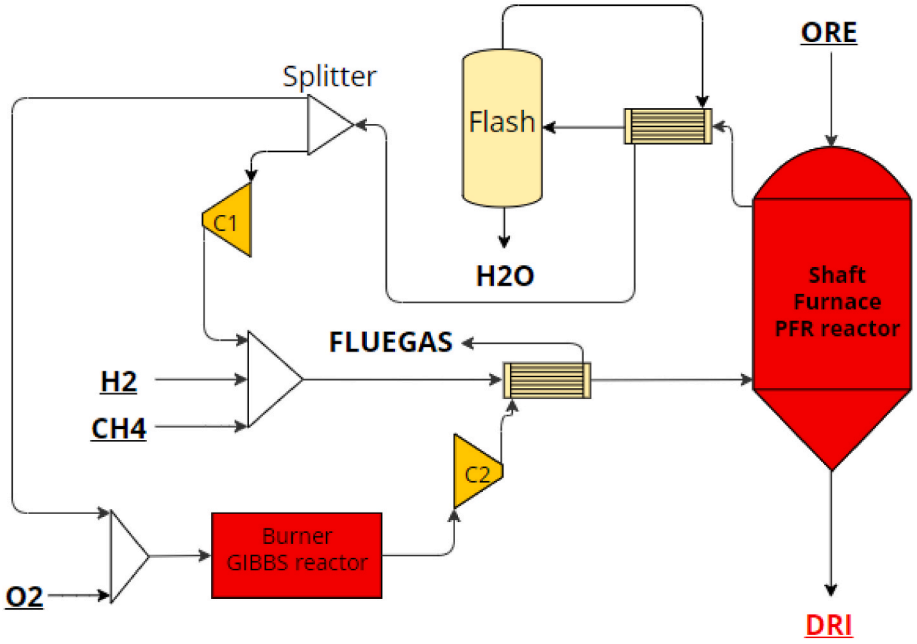

Fig. 3. DRI-H_2 Model Aspen scheme.

adiabatic PFR reactors. In the first PFR, all reduction reactions take place simultaneously with SMR and WGS. The second PFR models the last part of the reactor where iron carburization takes place. The PFRs are set in adiabatic mode. Reducing gas and iron ore are introduced in the PFR series. No data is available on the composition and characteristics of the solid feed in the plant, so a typical composition for the feed of a Midrex process is assumed (Midrexb), where 95% of the ore is hematite and the rest are impurities ($SiO_2 + Al_2O_3$).

There are also three compressors in the diagram (C1, C2, C3). The compressors, for this scheme and for all other compressors in the following cases, are modeled with a polyprotic efficiency of 0.75 and a mechanical efficiency of 0.96.

Finally, the solid furnace product, i.e. DRI, is sent to the EAF furnace section for conversion to steel. Hot charging of DRI (HDRI) is a proven method to effectively reduce the cost per ton of liquid steel. The product is then transported hot and fed directly to the EAF oven at a temperature of 600 °C. The main advantages of hot charging DRI in an EAF are twofold (Getting the Most From Direct Reduced Iron - Operational Results of MIDREX).

- Increased furnace productivity and reduced melting energy costs. Entering the solid at 600° compared to 25 results in energy savings, for the entire EAF furnace operation, of 25%. This translates into lower economic costs for energy purchase and lower CO_2 equivalent emissions (see Ch. 3.2.) (Duarte et al.).
- Reduction in the amount of pollutants.

2.4.1. DRI-NG-CCS

In achieving decarbonization goals (see Ch. 1), Carbon Capture is a solution worth considering. CCS solutions cannot be a final solution, but bridging solutions to reduce emissions in the meantime that green steelmaking technologies can make the progress to become technically and economically competitive.

CO_2 absorption is not an integral part of the steelmaking process. Carbon dioxide removal is not necessary in a MIDREX plant because the CO_2 is recycled back into the reformer and converted into carbon monoxide (Carbon Capture,). However, a CO_2 removal system can be included in these facilities if it is economically feasible (e.g., through carbon tax credits) and if there is a means of storing (CCS) or using the CO_2 (CCU).

An extensive study done in the literature by the authors, leads to the conclusion that very few production plants adopt CCS. Instead, there are several projects launched in recent years that include the startup of CCS pilot plants (Santos, 2014). CCS in the steel industry is a competition between Chemical Absorption (i.e., MDEA) vs Physical Adsorption (VPSA/PSA). Compared with other processes, amine absorption is currently regarded as the most economical technology for CO_2 capture (Dutcher et al., 2015). Methyl diethanolamine (MDEA) absorption is already one of the most widely used CO_2 capture solutions in industry, for capturing CO_2 from gaseous streams at high purity (CO_2 purity ~99.4%) (Santos, 2014), (Antonini et al., 2021) reaching removal efficiency up to 95% for carbon dioxide (MOFs amine scrubbing).

MIDREX company suggest including the CO_2 removal from the top gas fuel, which is used in the reformer for heating (see DRI-NG-CCS case in Fig. 2).

CO_2 removal is simulated with a separation unit to simplify the scheme. However, the energy consumption and the economic implications of the MDEA absorption process are discussed in detail in the following process analysis.

2.5. DRI-syngas model

Again, the reducing furnace and solid feed are the same as in the previous cases. What changes is the source and nature of the reducing gas. Gasification plant is the same as the previous case, but from which the produced syngas is taken instead of hydrogen. Syngas is cheaper than hydrogen, which must be separated from syngas by a pressure swing adsorption (PSA) unit to be obtained (Rispoli et al., 2021). At the same time, however, hydrogen has a higher energy content and, i.e. a better reducing agent than the syngas being considered. It is important, therefore, to examine the two schemes to see which solution is best suited for steel production.

The gas leaving the shaft is cooled and then sent to a flash where the water content is reduced. The gas stream is then split. One part is recirculated, and before being introduced into the furnace, Carbon dioxide is separated through an Acid Gas Removal unit (AGR) based on MDEA absorption (see Ch. 2.3.1). Also in this case, CO_2 removal is simulated with a separation unit to simplify the scheme. However, the energy consumption and the economic implications of the MDEA

absorption process are discussed in detail in the following process analysis.

The stream is then compressed and mixed with fresh syngas, heated and fed into the reduction furnace. The other part of the gas leaving the reduction furnace is sent along with air to a burner (Gibbs reactor, adiabatic mode, 1 bar) to provide heat to the reducing gas entering the furnace.

There are three compressors (C1, C2, C3) in the diagram.

2.6. DRI-H_2 model

The use of hydrogen as a reducing gas aims to reduce CO_2 emissions, decoupling production from the consumption of fossil resources. A DRI plant based entirely on hydrogen is slightly different from one based on natural gas, as it works with carbon-free compounds.

The reduction furnace and the solid feed are the same as the DRI-NG plant. Gases leaving the furnace, containing mainly water and unreacted hydrogen, are cooled, and then sent to a flash unit where the condensed water is purged. The stream from the flash is recirculated to the furnace together with a current of fresh hydrogen and methane. Before recirculation, the current from the flash must be split. Part of it is sent to a burner (Gibbs reactor, adiabatic mode, 1 bar) together with oxygen to generate the heat necessary to bring the reducing gas to the required temperature. Fresh hydrogen is manipulated to achieve the desired degree of metallization while methane is injected to allow carburization to take place. Even with the transition to fossil-fuel-free iron production technology, in which iron ore pellets are reduced exclusively by hydrogen, the incorporation of carbon (in the form of cementite) remains crucial or necessary in directly reduced iron. This is because it is crucial for the efficient and uninterrupted smelting of DRI during steelmaking processes (Sandeep Kumar et al).

Based on the mode of hydrogen production, two scenarios are presented.

- The hydrogen and oxygen that the system requires are supplied by an electrolyzer, not simulated in the flowsheet. The production of hydrogen by Alkaline Electrolyzer (AEL) is now an established technology and electrolysis plants with electrical power up to megawatts are commercially available (Grigoriev et al., 2020).
- The plant is coupled to a hydrogen production process from gasification of MSW (Municipal solid Waste), consisting of a certain aliquot of Refuse Derived Fuel (RDF) and a remaining part of Plasmix (non-Recyclable plastic) (Salman and Omer, 2020). The gasification process (as in the latter DRI-Syngas case) is not simulated, but the purchase price of the reducing gas is evaluated. The required oxygen is provided by an ASU (Air Separation Unit), not simulated in the flowsheet.

There are also two compressors (C1, C2) in the diagram.

2.7. EAF section model

HDRI from the reduction furnace, is then sent to the steel conversion section at 600 °C (see Fig. 4). The EAF operates with 100% HDRI. Fig. 5 shows the Aspen Plus scheme. The energy sources utilized in EAF include electricity and energy produced from oxidation reactions that occur during the refining process. Electrical energy is supplied via graphite electrodes and is usually the largest contributor in melting operations. To prevent cold spots in the eccentric furnace designs and enhance productivity when the transformer power is restricted, natural gas burners and carbon-oxygen injectors are employed to intensify the energy in the EAF. Lime is added to combine with the impurities and form slag. The EAF units produce liquid steel which can be treated in continuous casting and hot rolling mills units for the production of hot rolled coils. A stoichiometric reactor (RSTOIC) simulates the reactions occurring in the EAF at 1635 °C and 1 bar (Kirschen et al., 2021).

Table 4 reports the input flow rates to the EAF per ton of steel (see Table 5).

Limestone is used as a fluxing agent or a refining agent during the EAF steelmaking process. Calcium carbonate undergoes thermal decomposition into calcium oxide and carbon dioxide. All calcium carbonate is assumed to decompose, as in the following reaction:

$$CaCO_3 \rightarrow CaO + CO_2$$

In addition to the use of energy as a substitute for electricity, carbon sources are particularly used as foaming agents for slag (Echterhof, 2021). It is therefore assumed that all the carbon fed into the furnace that does not enter the steel is completely oxidized by oxygen.

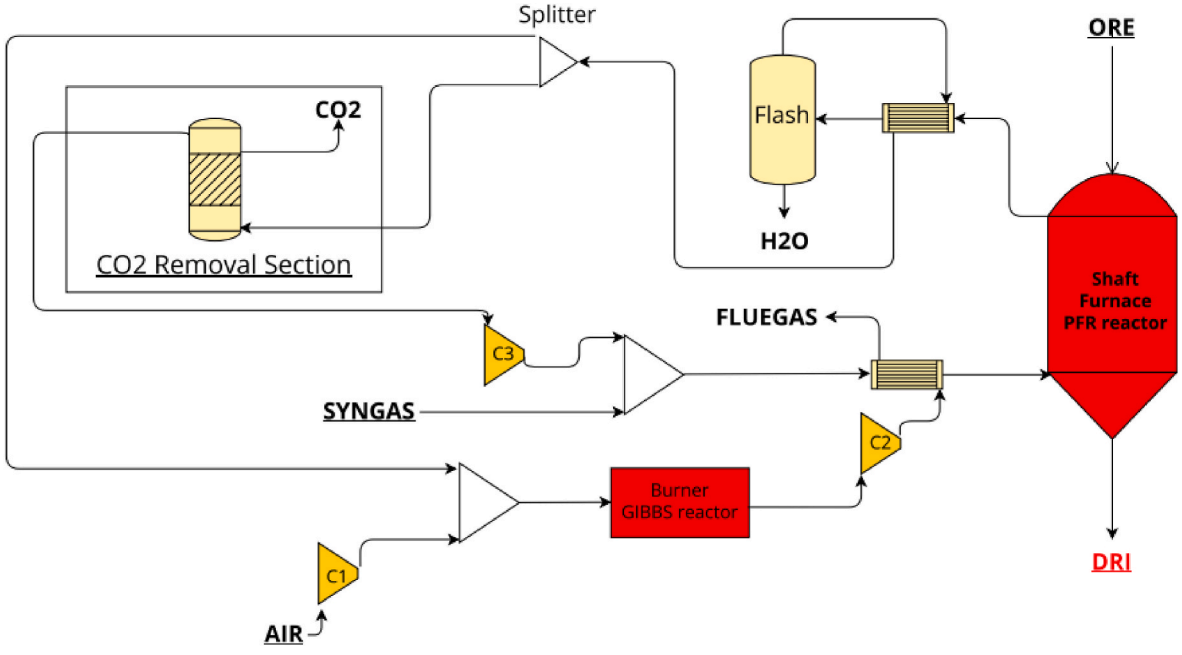

Fig. 4. DRI-Syngas Model Aspen scheme.

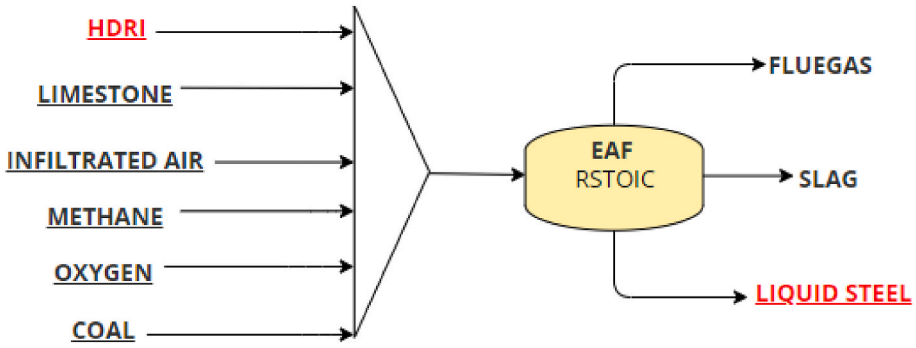

Fig. 5. EAF section scheme.

Table 4
Typical production parameters of EAF charges.

Methane	2	m^3/t	Kirschen et al. (2021)
Oxygen	35	m^3/t	Kirschen et al. (2021)
Coal and carbon fines	17	kg/t	Kirschen et al. (2021)
Infiltrated Air	150	kg/t	Kirschen et al. (2001)
Lime	50	kg/t	Manocha and Ponchon (2018)
Temperature	1635	°C	Kirschen et al. (2021)

Table 5
Specific power energy consumption.

	Power Energy Consumption	Unit	Reference
ASU	222	kWh/tO_2	Khallaghi et al. (2020)
EAF	450	kWh/t_{ls}	(Duarte et al.)
CO_2 absorber	200	kWh/tCO_2	Nayional Petroleum Council (2019)
AEL Electrolyzer	5	kWh/Nm^3 H_2	Grigoriev et al. (2020)
Casting	10.9	kWh/t_{ls}	Stanley (2013)

In the EAF graphite electrodes are consumed at a rate of 2 kg/t of liquid steel (resulting in further CO_2 emissions) (Remus et al., 2013) and costs of 4.32 $/kg are assumed for the electrodes (Vogl et al., 2018). The liquid steel casting is then processed in subsequent casting step. This step is not present in the simulation sheet, but operating and investment costs, energy consumption, and related CO_2 emissions are considered in subsequent analyses.

3. Process analysis

3.1. Energy analysis

The analysis target is to evaluate the global energy efficiency of the plant, considering all scenarios. Efficiency is calculated as reported in the following equation (Islam, 2018):

$$\eta_{en} = \frac{E_{prod}^{tot}}{E_{feed}^{tot}}$$

Where E_{prod}^{tot} and E_{feed}^{tot} [MW] are the total energy produced from the system and fed to the system, respectively. Efficiency can therefore be calculated as:

$$\eta_g = \frac{F_{Steel} \times LHV}{Net\ Power + \sum F_{in} \times LHV}$$

Where F [kg/s] represents the mass flowrate, LHV [MJ/kg] the Lower Heating Value and Net Power [MW] is the power energy required.

The following table shows the specific energy consumption of the units not simulated on Aspen Plus, but which are considered for process analysis.

3.2. Environmental analysis

Environmental analyses are aimed at highlighting the specific CO_2 emissions per ton of steel produced.

The emission calculations also encompass the corresponding CO_2 emissions linked to electricity generation, stemming from the utilization of externally sourced electricity.

For the calculation of the equivalent CO_2, the following emissions are considered.

- Power energy from the thermoelectrical production, only from fossil source, available on Italian territory, with an equivalent emission of 445.3 gCO_2/kWh (ISPRA).
- Renewable power energy, with zero equivalent CO_2 emissions.

CO_2 emissions for casting are 0.84 kg/t of liquid steel (Stanley, 2013).

3.3. Economic analysis

As a final analysis, the economic profitability of the scheme is evaluated for the different scenarios. It should also be underlined that the profitability analysis is performed without taking into account ore preparation and management of liquid steel casting from EAF section. The various required equipment specifications are considered in order to obtain the bare module cost (C_{BM}) also depending on the material chosen and the operating pressure (Turton et al.). Known C_{BM}, Total Module Cost (C_{TM}) is determined by the following relation:

$$C_{TM} = 1.18 \times \sum_{Equipment} C_{BM}$$

in which honorary and unforeseen fees are included (15% and 3% of total cost, respectively) (Turton et al.). Similarly, the Grass Roots Cost (C_{GR}), in which the costs of the auxiliary structures are also considered, increasing the C_{TM} only with the Bare Module Costs of the auxiliary equipment at the reference conditions (carbon steel material and atmospheric pressure), as these do not depend on operating pressure and material, through the relationship according to (Turton et al.):

$$C_{GR} = C_{TM} + 0.5 \times \sum_{Equipment} C_{BM}^{\circ}$$

In this analysis, it is considered as an approximation that the Fixed Capital Investment (FCI) coincides with the calculated Grass Roots cost, then considering the land cost for the physical construction of the plant to be $3 M, for all scenarios analyzed. For the determination of C_{OM} (cost of manufacturing), the costs of raw materials, labour, utilities (in particular power energy cost) and waste management have been

considered. Bare Module Cost of furnaces, compressors/funs are estimated based on reports given by Turton et al. For other equipment, more complex, such as shaft and EAF furnaces, Turton reports cannot be used. Therefore, specific investment costs, based on their cost attribute, found in the literature for individual units are used. Similarly, a casting plant that processes 4.3 million tons of steel has an investment cost of 195 M$ (Stanley, 2013). This cost is scaled by tons of steel by a factor of 0.6. In calculating the investment cost of the ASU unit, it is necessary to take the cost of the same unit in the literature as a reference and scale it according to size using a cost scaling factor (f) equal to 0.5 (Trinca et al., 2023) and actualize it according to the correct *Chemical Engineering Plant Cost Index* (CEPCI).

Returns from oxygen, in the case of electrolyzer use, are included in revenues. The assumptions by Pardo et al. (2012) that 60% of oxygen can be sold at a price of 65.7 $/t are adopted (Pardo and Moya, 2013).

Table 6 reports investment costs, purchase and sale price of materials and utilities.

A CEPCI of 750 (September 2021) is used. Commodity and energy prices are as up-to-date as possible and refer to the European market. From the study in the literature, it is evident that the gap between the cost of energy from fossil sources and renewable energy has narrowed substantially. But this is more due to the price increase for fossil resources rather than that of renewable energy. The general price increase has also affected steel, whose value has increased, favorably impacting the construction of CFD (Cash Flow Diagram).

In the case of EAF, Shaft Furnace and CO_2 Absorber equipment, a specific cost is provided, which depends on the quantity of tons processed in a single year (plant size).

Finally, the labour cost is assessed, considered among the variable costs of the plant, using the relationship reported extensively in the literature (Turton et al.):

$$N_{OL} = \left(6.29 + 31.7 \times P^2 + 0.23 \times N_{np}\right)^{0.5}$$

where P represents the phases that require solids handling, in the process, N_{np} are the number of employees for each equipment excluding pumps and tanks, while N_{OL} represents the number of operators per shift; considering 1095 shifts in a year (4.5 operator per shift). Labor costs are estimated by considering a gross salary for a steel worker in Italy of 50,000 $/y (Average Salary).

Cash Flow Diagram (CFD) is built on the base of: raw materials, labour, waste treatment cost and revenues of sales; 45% taxation, 10% interest rate and a plant construction time of 2 years. In all cases, MACRS (Modified Acceleration Cost Recovery System) amortization is considered, i.e. at a double decreasing rate over a period of 5 years with an interest rate of 10%; whereas the cost of the land is not included in depreciation for regulatory reasons. CFD is determined in the case of discounted analysis at 20 years of service life (Vogl et al., 2018) to evaluate the Payback Time Period (PBT), the Net Present Value (NPV) for the discounted analysis and finally the Return on Investment (ROI).

Table 6
Equipment investment cost and material price.

Equipment Investment Cost			
	Unit	C_{BM}	Reference
AEL	$/kW	972	Trinca et al. (2023)
EAF	$/($t_{STEEL}$/year)	160	Vogl et al. (2018)
Shaft Furnace	$/($t_{DRI}$/year)	250	Krü et al. (2020)
CO_2 Absorber	$/($t_{CO2}$/year)	22	Rochelle (2014)
ASU			
F	Base Cost (M$)	Year	Reference
0.5	40	2021	Trinca et al. (2023)
Materials Price			
	Unit	Cost	Reference
Iron Ore Pellet	$/t	45	(Iron Ore)
Methane	$/kg	0.64	(EU Natural Gas)
Demineralized Water	$/t	14.5	(Turton et al.)
Coal	$/t	135	(Coal PRICE)
Limestone	$/t	32.5	(Limestone Cost)
Syngas	$/kg	0.81	Rispoli et al. (2021)
H_2 MSW	$/kg	6.10	Rispoli et al. (2021)
Steel	$/t	844	(Steel Cost)
Oxygen	$/t	65.7	Pardo and Moya (2013)
Operative Cost			
Casting	$/$t_{HRC}$	16.25	Stanley (2013)
EAF graphite electrodes	$/$t_{HRC}$	8.64	Vogl et al. (2018)
Power Energy Price			
	Unit	Cost	Reference
Fossil Energy	$/MWh	146	(Electricity prices in Europe)
Renewable Energy	$/MWh	220	(Renewable-ilSole24ORE)

3.3.1. Monte Carlo simulation

The analysis described in the previous paragraph is done on the basis of raw material costs and utilities that are as up-to-date as possible to return a snapshot analysis. The results are useful for comparing different schemes, but it should be kept in mind that the costs of raw materials and electricity, however, are highly variable, particularly in recent months. To deepen the analysis and return more complete results a Monte Carlo analysis is conducted. Monte Carlo analysis is a computational technique that uses random sampling and statistical methods to model and analyze complex systems. Monte Carlo analysis helps in evaluating and managing risks. By modeling the system with random inputs, it is possible to identify the potential risks and their likelihoods. The purchase costs of methane, electricity, and the cost of selling steel are varied. In this way, it is possible to assess the probability of obtaining positive NPV, ROI, and PBT indices.

Costs are varied from the base value (Table 6) as follows.

- Methane: −50%; +460% (EU Natural Gas).
- Fossil power energy: −80%; +280% (Italy Electricity Price).
- Renewable power energy: −15% (Xiao et al., 2021).
- Steel: −59%; +84% (Steel Cost).

Ranges are established based on price histories found in the literature. As for renewable energy, it is acclaimed that between now and the next few decades its price will decrease (Xiao et al., 2021). Therefore, only values below the base value are considered in the Monte Carlo analysis.

4. Results and discussions

4.1. DRI-NG results and validation

The following Table 7 compares the model results with the experimental values reported in the literature.

Metallization is defined according to the following equation (Hosseinzadeh et al., 2022):

$$MD(\%) = \frac{Fe + Fe_3C}{Total\ Fe(Fe + FeO + Fe_3C)}$$

As already mentioned, the model is initialized by entering the same reducing gas current as in the literature.

A flow of 3110.4 kg/h of pure water vapor is separated at the scrubber (separation unit). The following splitter is manipulated to maintain a constant reducing gas flowrate at the furnace inlet equal to that reported in literature. The results show that 65% of the stream from the scrubber is recirculated to the reformer while the remainder is sent to the burner. This value reflects the ranges common to Midrex plants (Bechara et al., 2018), (Olayebi, 2014). The calorific value of the split stream is sufficient to provide the necessary heat for the reforming process. Therefore, there was no further addition of fresh methane to the reforming furnace burner. Thus, the total methane flow rate is 4340.58 kg/h, divided as follows.

Table 7
Comparison of the Gilmore data (Parisi and Laborde, 2004), (Shams and Moazeni, 2015), (Hosseinzadeh et al., 2022) with model prediction.

	Unit	Model	Gilmore Data	Difference (%)
Inlet reducing gas				
Flow rate	Nm^3/h	53,862.31	53,863	0
Temperature	°C	930	930	0
Pressure	bar	2.4	2.4	0
Composition				
H_2	%	51.93	52.58	1.24
CO	%	30.57	29.97	2.00
H_2O	%	4.81	4.65	3.44
CO_2	%	4.71	4.8	1.88
N_2 ($+CH_4$)	%	7.98	8.1	1.48
Outlet gas				
Flowrate	Nm^3/h	53,799.74	–	–
Temperature	°C	660	–	–
Composition				
H_2	%	36.98	37.00	0.05
CO	%	18.58	18.9	1.69
CO_2	%	15.51	16.10	3.66
H_2O	%	20.48	21.20	3.40
N_2 ($+CH_4$)	%	8.45	8.60	1.74
Solid				
Required Solid feed	t/h	37.30	–	–
DRI Production	t/h	27.16	26.40	2.97
Steel Production	t/h	25.29	–	–
DRI Composition				
Fe	%	84.23	–	–
FeO	%	7.06	–	–
Carbon	%	1.98	2	0.99
Gangue	%	6.46	6.3	2.54
Metallization	%	92.42	93	0.63

- 4014.86 kg/h to the reformer
- 288.77 kg/h to the combustion step with oxygen before the reduction furnace
- 36.18 kg/h to the EAF furnace

The composition at the shaft inlet therefore depends on the composition at the shaft outlet. This has led to an almost negligible difference in composition, at both the inlet and outlet of the reactor. However, simulation results are in excellent agreement with literature data.

The solid species composition profiles (Fig. 6) show that the first step of reduction from hematite to magnetite is extremely fast compared to the subsequent steps. Carburization, on the other hand, occurs mainly in the final part of the furnace as the iron concentration increases.

The 27.16 t/h of HDRI are then converted into steel in the EAF conversion section, from which 25.29 t/h of steel are produced.

The total methane and oxygen demand of the plant DRI-EAF is 171.57 and 72.38 kg/t of steel, respectively (Table 8).

As already mentioned, the DRI production plant requires three compressors for operation (Table 9). A fan can be used for unit C1 and C2.

To see the properties of all the flow rates of the various schemes, integrate the information in the Supplementary Material.

4.1.1. DRI-NG-CCS

The inclusion of the CO_2 removal unit allows 95% of the CO_2 to be recovered from the stream to be sent to the reformer furnace. Thus, 8.19 t/h of CO_2 are removed. This will be discussed in depth in the following analyses.

As a result, the results for C1 and C2 fans also change slightly (Table 10).

4.2. DRI-H_2 results

The shaft and solid feed retain the same properties as in the DRI-NG case. Even using pure hydrogen as a reducing agent, with the addition of a smaller proportion of methane for carburization, the DRI product retains the desired qualities (Table 11).

The total demand for hydrogen is 1.46 t/h, while that for oxygen is 2.65 t/h. Therefore, 57.62 kg of hydrogen are required for every ton of steel produced (Table 12). This value agrees with the work of Bhaskar et al., which estimates the hydrogen required at the electrolyzer as 59 kg/t_{STEEL}. Vogl et al. (2018) study, on the other hand, reported 51 kg/t_{STEEL}.

Compared with the DRI-NG process, a flash needs to be added to separate the water from the stream exiting the reduction furnace. The unit operates at 45 °C and a pressure of 1.4 bar and separates a stream of

Table 8
Specific Consumption DRI and EAF section.

	Specific Consumption	Unit
DRI Plant		
Methane	158.46	kg/t_{DRI}
Oxygen	20.87	kg/t_{DRI}
EAF Section		
Methane	1.43	kg/t_{STEEL}
Oxygen	49.97	kg/t_{STEEL}
Carbon	17	kg/t_{STEEL}
Limestone	50	kg/t_{STEEL}

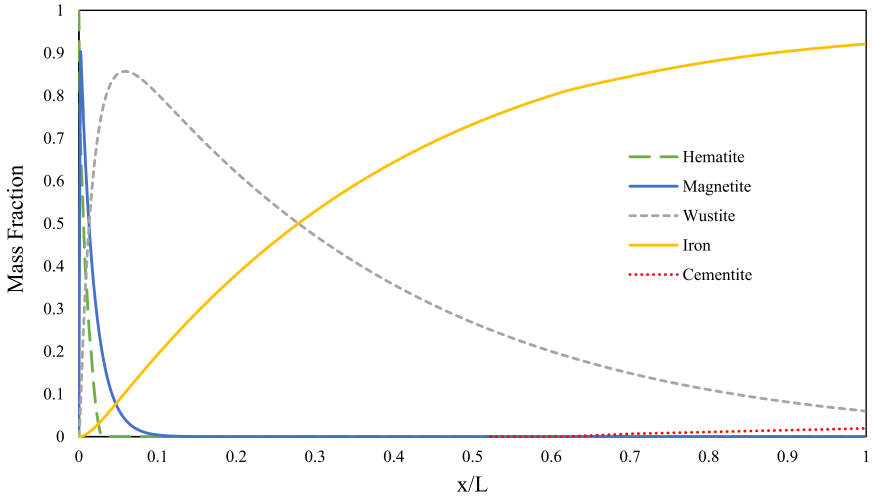

Fig. 6. Solid species mass fraction profiles along shaft furnace reduction section length (L = 9.75 m).

Table 9
Compressors results.

	Unit	C1	C2	C3
Discharge Pressure	bar	1.1	1.1	2.7
Pressure Ratio	–	1.1	1.1	1.93
Net Power Required	kW	146.61	1288.50	2870.96

Table 10
Compressors results.

	Unit	C1	C2	C3
Discharge Pressure	bar	1.1	1.1	2.7
Pressure Ratio	–	1.1	1.1	1.93
Net Power Required	kW	132.11	936.24	2870.96

11503.15 kg/h, containing 99.9% water.

To maintain the desired thermal profile within the reactor for the required degree of metallization to be achieved, it is necessary for the reducing gas stream to enter the reactor at a temperature of 1615 °C. This temperature is obviously higher than in the DRI-NG case, given the high endothermicity of the reduction by hydrogen. The heat required to reach this temperature is provided by the oxy-combustion of hydrogen. The high inlet temperature is difficult to sustain from a technical point of view (construction limits, materials, etc.). Methods to flatten the thermal jump within the reduction furnace should be investigated, such as increasing the number of injections and also evaluating oxygen injections.

The splitter must be set so that 82% of the stream is recirculated to the shaft, while the remaining is burnt.

Table 13 shows the results of the compressors. The results of the C2 unit recommend using a fan.

Table 11
DRI-H_2 results.

Inlet Reducing Gas		
Flow rate	Nm^3/h	25,501.40
Temperature	°C	1615
Pressure	bar	2.4
Composition		
H_2	%	98.2
CH_4	%	0.34
H_2O	%	1.46
CO_2	%	10^{-3}
Outlet Gas		
Flowrate	Nm^3/h	25,564.18
Temperature	°C	660
Composition		
H_2	%	42.15
CH_4	%	0.10
H_2O	%	57.75
CO_2	%	10^{-3}
Solid		
Required Solid feed	t/h	37.30
DRI Production	t/h	27.16
Steel Production	t/h	25.30
DRI Composition		
Fe	%	84.55
FeO	%	6.74
Carbon	%	1.99
Gangue	%	6.47
Metallization	%	92.77

Table 12
Specific Consumption DRI and EAF section.

	Specific Consumption	Unit
DRI Plant		
Hydrogen	53.67	kg/t_{DRI}
Oxygen	50.97	kg/t_{DRI}
Methane	1.77	kg/t_{DRI}
EAF Section		
Methane	1.43	kg/t_{STEEL}
Oxygen	49.97	kg/t_{STEEL}
Carbon	17	kg/t_{STEEL}
Limestone	50	kg/t_{STEEL}

4.3. DRI-syngas results

Again, the nature of the reducing gas does not affect the quality of the product (Table 14).

The total demand for Syngas is 13.38 t/h, 529.79 kg for every ton of steel produced (Table 15).

The splitter must be set so that 80% of the stream is recirculated to the shaft, while the remainder is burnt to give the necessary heat to the incoming reducing gas.

Table 16 shows the results of the compressors. Given the low heads and flow rates required, it is sufficient to use two fans, for C1 and C2 units.

Also in this case, the flash unit operates at 45 °C and a pressure of 1.4 bar and separates a stream of 6434.14 kg/h, containing 99.6% water. The AGR unit processes a gas flow rate of 56548.18 Nm^3, separating 7514.37 Nm^3 of pure CO_2.

4.4. Energy analysis

Table 17 shows the electricity consumption of each individual unit for all analysed schemes. For a better understanding of energy consumption, specific energy consumption is estimated (Table 18). The disadvantage, in terms of consumption, due to the adoption of the absorption unit is really small: indeed, it saves power absorbed at fans C1 and C2. In DRI-H_2 case, thermal energy consumption is given by methane and carbon flows. The heat flow due to fresh hydrogen entering the cycle is already included in the electrical energy consumption, since the electricity expenditure to produce it is calculated. The results show that the plant with hydrogen from electrolyzer system has higher energy consumption than the other cases. In particular, the high electricity demand of the hydrogen plant stands out. This is due to the high consumption of electrolyzer. The case with syngas shows similar consumption to the one with methane.

The calculation of efficiencies (Table 19) is useful for evaluating the energy performance of different plants.

The energy efficiencies show that the hydrogen from electrolyzer plant has a lower energy performance than the other two schemes. This is due to the high energy consumption of the electrolyzer affecting the overall performance. The DRI-NG and DRI-Syngas/DRI-H_2 MSW schemes have similar efficiency. In the DRI-NG case, the efficiency evaluation is also affected by the methane reforming step for conversion to syngas, requiring energy by increasing thermal energy consumption. In the DRI-Syngas and DRI-H_2 MSW cases, however, the MSW gasification step for producing the reducing gas is not included in the plant scheme. From this it can be seen that even though the three schemes have similar overall efficiencies, the DRI-NG scheme is more efficient, due to the use of methane, which results in a better-quality reducing gas, and the many optimizations made, including based on solutions provided by the manufacturers. Of course, it should be considered that the simulations work in ideal situations. In the complexity of reality, the efficiencies are lower. Be that as it may, the results of the analysis are a good method for a comparison between different schemes.

Table 13
Compressors results.

	Unit	C1	C2
Discharge Pressure	bar	2.4	1.1
Pressure Ratio	–	1.8	1.1
Net Power Required	kW	2940.98	165.67

Table 14
DRI-syngas results.

Inlet Reducing Gas		
Flow rate	Nm^3/h	62,590.3
Temperature	°C	918.45
Pressure	bar	2.4
Composition		
H_2	%	42.12
H_2O	%	3.33
CO	%	42.55
CO_2	%	3.01
N_2+ CH_4	%	8.9
Outlet Gas		
Flowrate	Nm^3/h	62,676.86
Temperature	°C	660
Composition		
H_2	%	29.51
H_2O	%	16.12
CO	%	32.42
CO_2	%	13.09
N_2+CH_4	%	8.6
Solid		
Required Solid feed	t/h	37.30
DRI Production	t/h	27.13
Steel Production	t/h	25.27
DRI Composition		
Fe	%	84.87
FeO	%	6.34
Carbon	%	2.00
Gangue	%	6.49
Metallization	%	93.19

Table 15
Specific Consumption DRI and EAF section.

	Specific Consumption	Unit
DRI Plant		
Syngas	493.09	kg/t_{DRI}
EAF Section		
Methane	1.43	kg/t_{STEEL}
Oxygen	49.97	kg/t_{STEEL}
Carbon	17	kg/t_{STEEL}
Limestone	50	kg/t_{STEEL}

Table 16
Compressors results.

	Unit	C1	C2	C3
Discharge Pressure	bar	1.1	1.1	2.5
Pressure Ratio	–	1.1	1.1	2.27
Net Power Required	kW	9.24	164.93	2257.52

Table 17
Power energy consumption.

	Unit	DRI-NG		DRI-H_2	DRI-Syngas	DRI-H_2 MSW
		No CCS	CCS			
Compressors	MW	4.31	3.94	3.11	2.43	3.11
EAF	MW	11.32	11.32	11.38	11.37	11.38
ASU	MW	0.36	0.36	–	–	0.61
AEL	MW	–	–	81.04	–	–
Casting	MW	0.27	0.27	0.27	0.27	0.27
CO_2 Absorber	MW	–	1.64	–	2.93	–
Total	MW	16.26	17.53	95.8	17	15.37

4.5. Environmental analysis

Based on the results of the simulations and energy analyses, CO_2 emissions can be determined (Table 20). Total emissions are given by those from the process, i.e., the reduction and combustion step, and the equivalent emissions from electricity consumption.

The configuration that adopts pure hydrogen from fossil sources returned the largest carbon dioxide emission flowrate, mainly due to the equivalent fraction (131% more than DRI-NG case). Whereas the adoption of MSW syngas returned the largest process-CO_2 emission flowrate, with a total value that is 42% higher than in the DRI-NG case. This is mainly due to the composition in the reducing gas, resulting unbalanced toward CO compared to hydrogen (see Table 3 of MSW syngas composition). This leads to a higher CO_2 production in the reduction and combustion step. Better results may be obtained by including a pre-treatment of the MSW syngas before sending it to the DRI unit: this of course will lead to an increase of both CapEx and OpEx. However, the CO_2 stream that is separated in the absorption section, having a purity of more than 99%, would already be ready for storage. In the case where CO_2 is stored, it is possible to reduce emissions by 54%, obtaining a total emission of 12.65 t/h and a specific emission of 500.72 $kgCO_2/t_{STEEL}$. The use of hydrogen from gasification, instead of syngas, as is easy to predict, allows for a further reduction in CO_2 emitted.

For better understanding, the total specific $kgCO_2$/t of DRI and steel produced are shown in Table 21.

The specific CO_2 emissions of a DRI/EAF plant fall within the range 630–1150 $kgCO_2/t_{STEEL}$ (Kirschen et al., 2011b). Millner et al. reported a value of 777 $kgCO_2/t_{STEEL}$, while Strezov et al. (2013) reported 400 $kgCO_2/t_{DRI}$ for the DRI process alone.

The calculated DRI-H_2 plant emissions are also found to be in good agreement with the data reported in the literature. References (Cavaliere, 2019), (Carpenter, 2012) report an emission of 71 $kgCO_2/t_{STEEL}$.

As mentioned above, CO_2 emissions are reduced through appropriate optimizations and energy recoveries that minimized methane consumption. The adoption of CCS leads to a substantial reduction in CO_2 emission for the DRI-NG scenario (direct emissions, i.e. of Scope 1, decreases of about 40%). Obviously, on the other hand, the indirect emissions (equivalent, or of Scope 2) undergo a slight increase, because of the energy consumption in the reboiler of the stripper of the CCS system. Depending on the final use of the captured CO_2, additional costs of compression, storage and/or transport will have to be considered.

A separate discussion deserves the case with hydrogen. The use of hydrogen allows to cut down the CO_2 emissions associated with the process. In the case of full fossil energy use (worst case), the DRI-H_2 plant emits, due to high CO_2 equivalent emissions, 131% more than DRI-NG, making the plant environmentally unfavorable. Renewable energy also cuts down equivalent emissions, reducing them to zero. With full use of renewable energy (best case), emissions are reduced by up to 87%. Unfortunately, as is well known, at present it is not conceivable to be able to work all hours of the day and year with renewable energy. It will therefore be necessary to supplement energy from the grid. A common Midrex plant can work until 8000 h per year (MIDREX® Direct Reduction Plants). Considering 8 h per day of renewable energy, about 31% (2500 h) of the 8000 h can be covered. In this case, there is a specific CO_2 emission of 1255.77 $kgCO_2/t_{STEEL}$, about 63% more than in the DRI-NG case. To have an environmental benefit, and thus have an emission of less than 700 $kgCO_2/t_{STEEL}$, it is necessary for the plant to work at least 5136 h per year with renewable energy (see Fig. 7).

4.6. Economic analysis

With the results of the simulations, it is possible to determine the total investment for the purchase of the main equipment (Table 22). The DRI-H_2 plant has the highest investment cost, as is easy to expect given the high costs involved in purchasing the electrolyzer. The syngas and hydrogen plants from gasification are expected to have a lower

Table 18
Specific energy demand.

	Unit	DRI-NG			DRI-H_2		DRI-Syngas	DRI-H_2 MSW
		No CCS		CCS	Reference (Vogl et al., 2018), (Chiappinelli et al., 2020)	Model		
		Reference (Chiappinelli et al., 2020)	Model					
Electric	GJ/t_{STEEL}	2.5	2.33	2.51	>10.6	13.71	2.43	2.20
Thermal	GJ/t_{STEEL}	10.5	9.87	9.87	<1.9	1.39	10.8	8.30
Total	GJ/t_{STEEL}	13	12.20	12.38	12.5	15.10	13.23	10.20

Table 19
Energetic efficiency.

	Unit	DRI-NG		DRI-H_2	DRI-Syngas	DRI-H_2 MSW
		No CCS	CCS			
Inlet Thermal Energy	MW	547.18	547.18	536.64	554.39	536.64
Product Thermal Energy	MW	330.06	330.06	331.76	331.57	331.76
Power Energy	MW	16.26	17.53	95.8	17	15.37
η_g	%	58.58	58.45	52.46	58.03	60.10

investment cost. Once again, however, it must be considered that ready-to-use reducing agent is fed directly into the plant, while for the other processes it is also necessary to purchase the units (reformer, electrolyzer) for converting the raw material (methane, water) into reducing gas.

The investment cost of the DRI-NG plant is higher than what the reference (IEA G20 Hydrogen Report: Assumptions) reports, which estimates a cost of 119 M$, while it is less than 218 M$, as reported by the reference (Global Hydrogen Review). The increase in the investment cost of adopting CCS, is extremely small. This is in line with what is reported in the literature where a maximum increase of 8% is estimated (IEA G20 Hydrogen Report: Assumptions).

According to the reference (IEA G20 Hydrogen Report: Assumptions), a DRI-H_2 plant of equal capacity to the one modeled has an investment cost of 191 M$ (casting investment costs are not included). For the same plant, Gielen et al. estimates an investment cost of 285 M$, while Rosner et al., 2023 245 M$.

To construct the cash flow diagrams, annual costs and revenues are defined for the four plants (Table 23). For all cases, the labor cost is very similar. This is explained in the fact that presiding over the labor cost calculation is all equipment where solids handling takes place, and the number of the latter does not vary for the plants.

Based on the calculation of the investment cost of the main equipment, it is possible to define discounted CFD (Fig. 8). Only the CFD of the DRI-NG and DRI-NG-CCS are shown. As shown in Tables 22 and 23, even when the investment cost is lower (DRI-Syngas) than other schemes, the high cost of electricity and the purchase cost of raw materials lead to a negative NPV index. Because of this, hydrogen and syngas plants have all negative economic indices, thus making the plants economically unviable. Hydrogen from gasification has a higher cost than syngas, but due to the fact that hydrogen has a higher reducing potential the required mass flow rate is largely lower, leading to a lower annual cost to purchase hydrogen than syngas. Be that as it may, the low ROI, does not allow for a positive NPV at the end of the plant life.

The analyses developed show not high profits (even in cases of positive NPVs) against the necessary investments. It should be considered that these analyses are affected by the high variability in commodity, energy and money costs that has marked the economy since the COVID 19 pandemic. In addition, the European market has been strongly affected by higher prices and inflation due to the war in Ukraine. In contrast, the U.S. market, which is not dependent on imports from Russia, has not been affected by the Ukraine war crisis as Europe has been. Therefore, it is useful to see what the economic results would be using the cost of methane and electricity from the U.S. market (Table 24).

The cost of natural gas is about 0.5 fold than European one while electricity is just over half. Table 25 summarizes the economic indices of the same scenarios already examined but using U.S. methane and power energy costs. The results make it clear that steel production by DRI technology is highly dependent on the cost of energy (methane + electricity). Seeing how the rising price of them makes it economically

Table 20
CO_2 emissions.

		Unit	DRI-NG		DRI-H_2		DRI-Syngas	DRI-H_2 MSW
			No CCS	CCS	Fossil	Renewable		
Equivalent CO_2	DRI	tCO_2/h	2.08	2.64	37.47	–	2.26	1.65
	EAF + Casting	tCO_2/h	5.16	5.16	5.19	–	5.19	5.19
	TOTAL	tCO_2/h	7.24	7.8	42.66	–	7.45	6.84
Process CO_2	DRI	tCO_2/h	9.81	1.61	0.01	0.01	17.69	0.01
	EAF + Casting	tCO_2/h	2.44	2.44	2.43	2.43	2.44	2.44
	TOTAL	tCO_2/h	12.25	4.05	2.44	2.44	20.13	2.45
Total CO_2		tCO_2/h	19.49	11.85	45.1	2.44	27.58	9.29

Table 21
Carbon footprint factors.

	Unit	DRI-NG		DRI-H_2		DRI-Syngas		DRI-H_2 MSW
		No CCS	CCS	Fossil	Renewable	No CCS	CCS	
Specific CO_2	$kgCO_2/t_{DRI}$	437.73	156.47	1379.81	0.37	735.32	191.71	61.11
	$kgCO_2/t_{STEEL}$	770.43	468.42	1782.74	96.45	1091.59	500.72	367.22

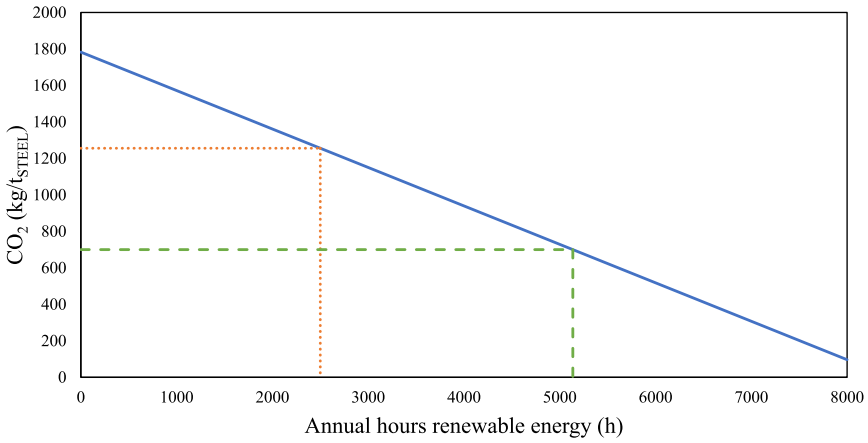

Fig. 7. CO_2 emissions in function of the working hours of renewable energy.

Table 22
Investment costs results.

	Investment Costs (M$)					
	DRI-NG		DRI-H_2	DRI-Syngas		DRI-H_2 MSW
	No CCS	CCS				
Shaft Furnace	54.36	54.36	54.32	54.16		54.32
EAF Furnace	32.20	32.20	32.26	32.26		32.26
C1	0.11	0.11	9.72	0.01		9.72
C2	0.76	0.63	0.12	0.12		0.12
C3	9.57	9.57	–	8.27		–
Reformer	4.62	4.62	–	–		–
Reformer Furnace	25.80	25.80	–	–		–
Furnace	–	–	9.91	7.59		9.91
Electrolyzer	–	–	78.78	–		–
CO_2 Absorber	–	1.45	–	2.58		–
ASU	13.06	13.06	–	10.84		15.98
Casting	32.44	32.44	32.47	32.44		32.47
Total (FCI)	172.92	174.24	217.58	148.27	154.78	

Table 23
Annual costs (Base value).

Cost (M$/y)					
	DRI-NG		DRI-H_2	DRI-Syngas	DRI-H_2 MSW
Raw Materials					
Iron Ore Pellet	13.43		13.43	13.43	13.43
Limestone	0.33		0.33	0.33	0.33
Methane	23.53		0.46	0.20	0.46
Carbon	0.46		0.46	0.46	0.46
Demineralized Water	–		1.56	–	–
Syngas	–		–	86.18	–
H_2-MSW	–		–	–	71.13
Product Materials					
Steel	170.15		170.15	170.15	170.15
Oxygen	–		2.88	–	–
Power Energy					
Fossil	No CCS	CCS	111.89	19.86	17.95
	18.99	20.48			
Renewable	–		168.61	–	–
Casting	3.24		3.24	3.24	3.24
EAF graphite electrodes	1.82		1.82	1.82	1.82
Labour					
	No CCS	CCS	4.19	4.19	4.19
	4.19	4.20			

difficult to produce steel, should make governments and companies think about how necessary it is also economically, and not only environmentally, to free themselves from the use of fossil. Particularly where, as in Europe, the cost of fossil is high.

The analyses also do not take into account, eventual carbon tax. The introduction of new carbon tax at the European level, would make less unfavorable production technologies with less environmental impact (DRI-H_2) and technologies where waste reuse takes place (DRI-MSW), whose emissions are exempt from taxation. To this end, a sensitivity analysis is conducted to see how a possible carbon tax impacts the economic performance of the DRI-NG plant (the only one that would be subjected to a carbon tax) (Fig. 9). The carbon tax applies to the direct emissions of the plant, not to the equivalent emissions.

The DRI-NG plant is more susceptible to the introduction of carbon tax, being more emissive. The inclusion of carbon tax makes the application of absorption more competitive than its non-use. In addition, as the cost of carbon tax increases, the disadvantage of using green technologies such as the DRI-H_2 plant is reduced.

4.6.1. *Monte Carlo simulation*

The results of Monte Carlo simulations help to get a more complete overview of the risks-benefits of investing in the technologies studied.

From the cumulative curves it is possible to infer the probability of having a positive NPV. For the DRI-NG and DRI-NG-CCS case, there is a positive NPV in around 45% of the cases (Fig. 10b). This shows that the investment has a high risk, which depends more on the cost of methane and energy. On the other hand, when energy costs remain low, they allow for a decent margin of return. In contrast, the production of steel using hydrogen from electrolysis has no economic advantage when using only green energy (Fig. 10d and e). CFD analysis clarifies the economic weight that renewable energy use, in DRI-H_2 plant, has on economic indices. As the use of renewables increases, the NPV decreases. It is interesting to note that directly using hydrogen from MSW gasification pays off compared to using syngas. Hydrogen costs more than syngas (because of the additional purification step) but being a better reducing agent the required flow rate is lower leading to better economic results.

5. Conclusions

The steel sector is facing the grade challenge of cutting its CO_2 emissions. The model of the entire DRI-EAF plant, based on kinetic considerations, validated on data from the Midrex GILMORE plant, allows the environmental impact of different kinds of reducing gases to be assessed, remaining unchanged in the quality of the product.

The plant adopting syngas from methane reforming is confirmed to

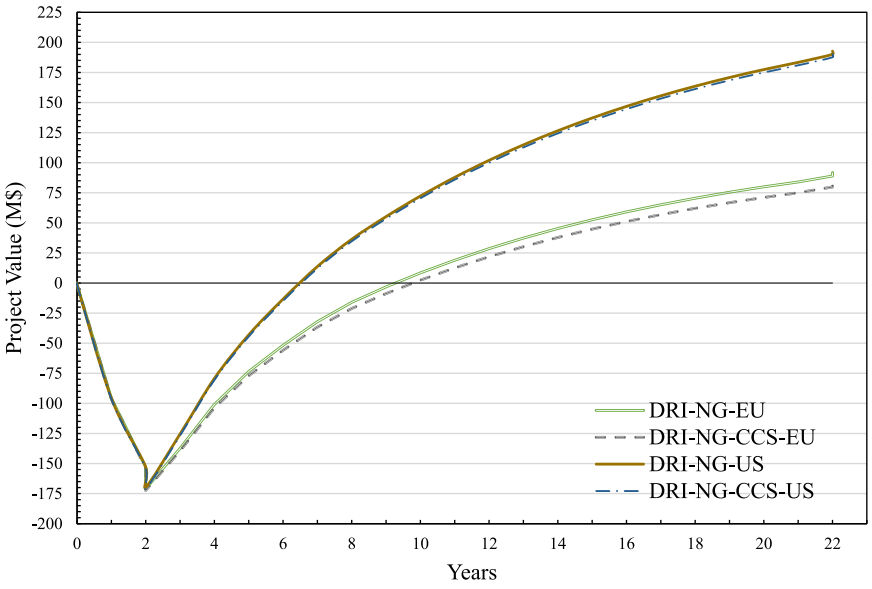

Fig. 8. Discounted CFD: DRI-NG and DRI-NG-CCS cases.

Table 24
U.S. methane and energy cost.

	Unit	Cost	Reference
Methane	$/kg	0.32	(United States Natural Gas Industrial Price)
Fossil Energy	$/MWh	81.5	(U.S. Energy Information Administration (EIA))

Table 25
CFD Results (DRI-NG and DRI-NG-CCS cases).

	Unit	EU Market		U.S. Market	
		No CCS	CCS	No CCS	CCS
NPV	M$	91.8	82.7	192.75	190.29
ROI	%	0.17	0.17	0.24	0.24
PBT	y	5.8	6.1	3.84	3.89

be the best performing, given the greater maturity of it compared to the other schemes. Although it has made significant reductions in CO_2 emissions compared with BF-BOF technology, it is with the use of renewable energy and green hydrogen from electrolyzer that greenhouse gas emissions can be cut down almost completely. In this direction, it is important to improve the efficiency of the plant, especially the electrolyzer.

The use of syngas and hydrogen from gasification of MSW allows the coupling of the steelmaking plant with a waste material upgrading plant. The environmental analysis reveals how the syngas scenario is highly emissive in terms of CO_2. This is due to the lower quality of the reducing gas, and its higher carbon monoxide content generating more CO_2 in the reduction and combustion steps and affecting the energetic efficiency. More than 60% of the CO_2 produced comes from the separation step and is already ready for eventual storage (additional energy and economic costs of power compression and its storage should be considered). Carbon capture and storage can lead the syngas plant to reduce emissions by up to 35% compared to the case with methane. Improving the product of

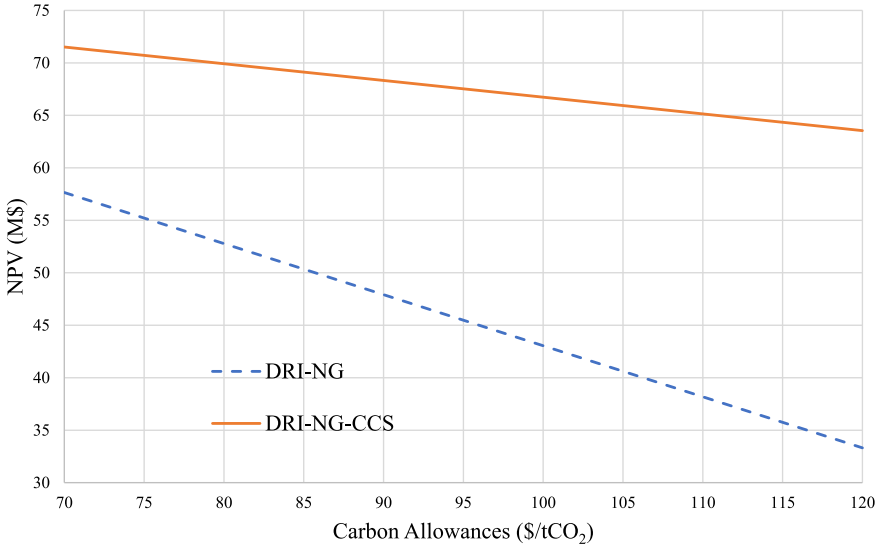

Fig. 9. NPV in function of Carbon Allowances price (EU Market).

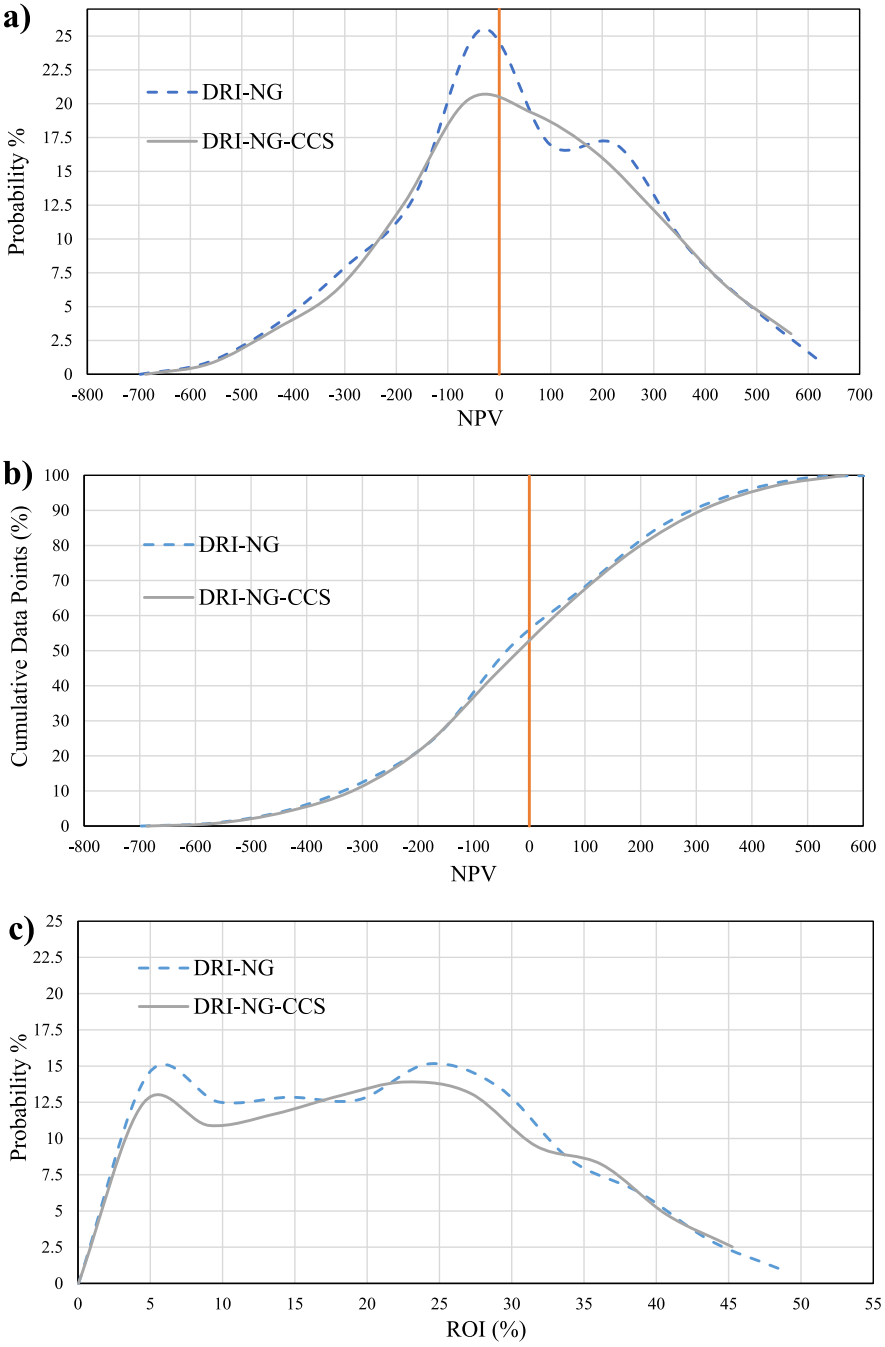

Fig. 10. Monte Carlo simulation results: a), b), c) DRI-NG and DRI-NG-CCS plants; d), e) DRI-H_2, DRI-H_2-MSW and DRI-Syngas plants.

MSW gasification by separating hydrogen from the gasification product leads to better environmental performance, with 27% lower emissions than the DRI-Syngas case with storage. In addition, the CO_2 emissions due to the reduction step come from the reuse of a waste anyway, and thus are to be considered neutral in the overall GHG balance and exempt from any carbon tax impositions. The real obstacle of using syngas from gasification is economic. Analysis show that the plant, due to the cost of syngas production, has low profitability. This is due to the cost of producing such syngas and the high demand for the plant, since it does not possess excellent quality as a reducing agent. Therefore, the use of syngas remains an economically risky option unless the cost of gasification of municipal solid waste is reduced and the efficiency of its use in the plant is increased. The use of hydrogen from gasification, on the other hand, provides a significant reduction in CO_2 emissions and in annual costs leading to a positive NPV at the end of the plant's life in 40% of the cases examined in the Monte Carlo analysis.

The work done, however, shows that the use of green hydrogen for steel production is still too dependent on the cost of renewable energy and on the efficiency of the electrolyzer, which causes high power consumption. Certainly, any economic incentives from government institutions will play a key role.

Analyses show the potential of alternative technologies to fossil fuel. In addition to the environmental aspect, the introduction of carbon tax, and rising prices of fossil resources is making it even more necessary to

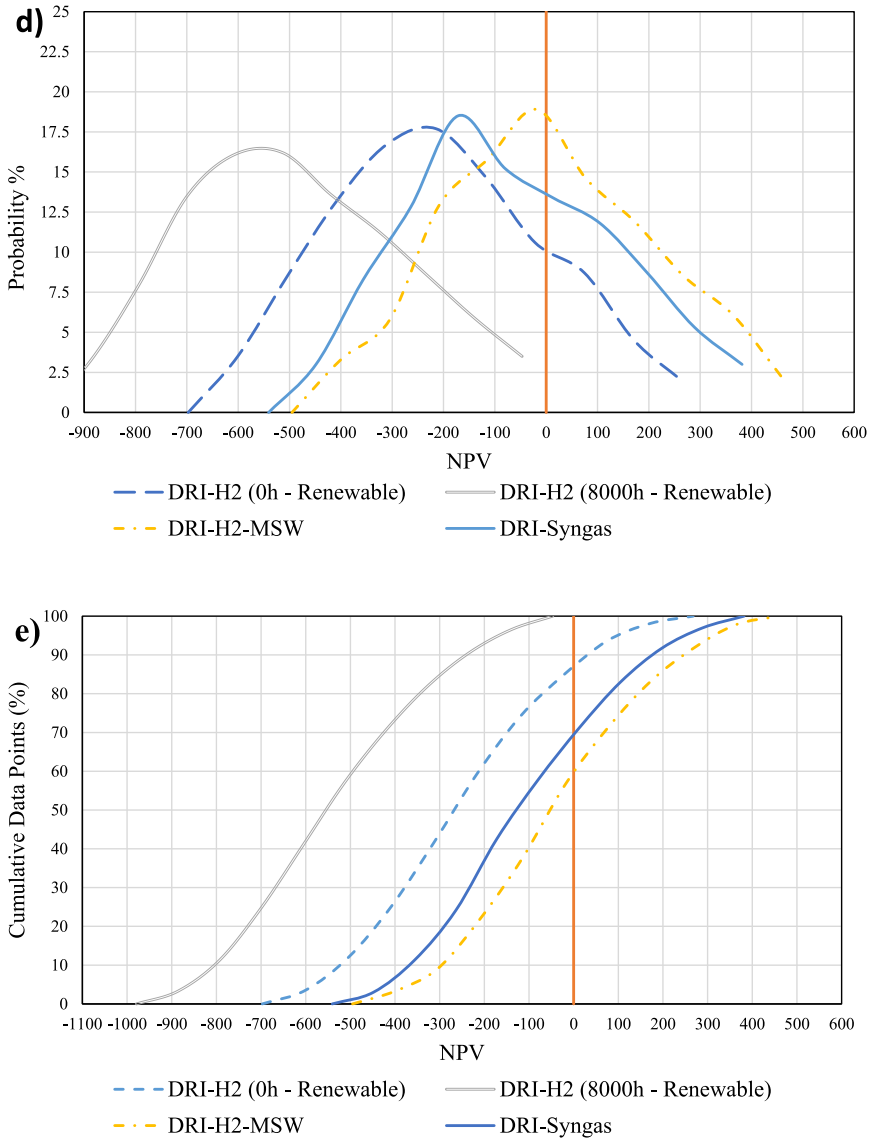

Fig. 10. (*continued*).

use green technologies. While waiting for these technologies to be deployed on a large scale, CCS is a viable solution to reduce emissions and reduce the economic impact of carbon tax.

The developed study aims to provide a validated model of the entire steelmaking process by direct reduction that can allow comparison of reducing gases of different nature, from energy, environmental and economic points of view. In future work, the model may be used for new additional green reducing gases, such as ammonia.

Future work should optimize the distribution of hydrogen injection points in the DRI-H_2 furnaces, evaluating any oxygen injections, to improve the thermal profile inside the furnace and provide a sensitivity analysis on increasing electrolysis load factor by analyzing hydrogen storage scenario, to allow a higher use of renewable energy.

CRediT authorship contribution statement

Antonio Trinca: Methodology, Software, Writing – original draft, Conceptualization. **Daniele Patrizi:** Software. **Nicola Verdone:** Supervision. **Claudia Bassano:** Supervision, Conceptualization. **Giorgio Vilardi:** Supervision, Writing – review & editing, Investigation.

Declaration of competing interest

The authors declare that they have no known competing financial interests or personal relationships that could have appeared to influence the work reported in this paper.

Data availability

Data will be made available on request.

Appendix A. Supplementary data

Supplementary data to this article can be found online at https://doi.org/10.1016/j.jclepro.2023.139081.

References

Global Hydrogen Review"Global Hydrogen Review: Assumptions Annex".
Alhumaizi, K., Ajbar, A., Soliman, M., 2012. Modelling the complex interactions between reformer and reduction furnace in a midrex-based iron plant. Can. J. Chem. Eng. 90 (5), 1120–1141. https://doi.org/10.1002/cjce.20596.

Antonini, C., Pérez-Calvo, J.F., van der Spek, M., Mazzotti, M., 2021. Optimal design of an MDEA CO2 capture plant for low-carbon hydrogen production — a rigorous process optimization approach. Sep. Purif. Technol. 279 https://doi.org/10.1016/J.SEPPUR.2021.119715. Dec.

Aslam, R., Usman, M.R., Irfan, M.F., 2016. A comparative study of LHHW and ER kinetic models for NO oxidation over Co3O4 catalyst. J. Environ. Chem. Eng. 4 (3), 2871–2877. https://doi.org/10.1016/j.jece.2016.05.035.

M. Atsushi, H. Uemura, and T. Sakaguchi, "MIDREX Process ," Plant Engineering Department, Iron Unit Division, Natural Resources & Engineering Business.

Basson Edwin, "2022 World Steel in Figures", [Online]. Available: https://worldsteel.org/wp-content/uploads/World-Steel-in-Figures-2022.pdf.

Bechara, R., Hamzeh, H., Mirgaux, O., Patisson, F., 2018. Optimization of the iron ore direct reduction process through multiscale process modeling. Materials 11, 1094.

A. Bhaskar, M. Assadi, and H. N. Somehsaraei, "Decarbonization of the Iron and Steel Industry with Direct Reduction of Iron Ore with Green Hydrogen", doi: 10.3390/en13030758.

Carpenter, A., 2012. CO 2 Abatement in the Iron and Steel Industry.

Cavaliere, P., 2019. Clean Ironmaking and Steelmaking Processes. Springer International Publishing. https://doi.org/10.1007/978-3-030-21209-4.

Chiappinelli, O., et al., 2020. A Green COVID-19 Recovery of the EU Basic Materials Sector: Identifying Potentials, Barriers and Policy Solutions. Deutsches Institut für Wirtschaftsforschung. Mar. 17, 2023. [Online]. http://www.diw.de/discussionpapers.

Deng, L., Adams, T.A., 2020. Techno-economic analysis of coke oven gas and blast furnace gas to methanol process with carbon dioxide capture and utilization. Energy Convers. Manag. 204, 112315 https://doi.org/10.1016/J.ENCONMAN.2019.112315.

Dhawan, N., Manzoor, U., Agrawal, S., 2022. Hydrogen reduction of low-grade banded iron ore. Miner. Eng. 187 https://doi.org/10.1016/j.mineng.2022.107794.

P. Duarte, T. Scarnati, and J. Becerra, "ENERGIRON Direct Reduction Technology-Economical, Flexible, Environmentally Friendly".

Dutcher, B., Fan, M., Russell, A.G., 2015. Amine-based CO2 capture technology development from the beginning of 2013-A review. ACS Appl. Mater. Interfaces 7 (4), 2137–2148. https://doi.org/10.1021/AM507465F. Feb.

Echterhof, T., 2021. Review on the use of alternative carbon sources in EAF steelmaking. Metals 11 (2). https://doi.org/10.3390/met11020222. MDPI AG, pp. 1–16, Feb. 01.

I. Energy Agency, "Global Energy Rewiev 2021," 2021, [Online]. Available: https://iea.blob.core.windows.net/assets/d0031107-401d-4a2f-a48b-9eed19457335/GlobalEnergyReview2021.pdf.

Ernst, D., Manzoor, U., Souza Filho, I.R., Zarl, M.A., Schenk, J., 2023. Impact of iron ore pre-reduction degree on the hydrogen plasma smelting reduction process. Metals 13 (3). https://doi.org/10.3390/met13030558. Mar.

D. Gielen, D. Saygin, E. Taibi, and J.-P. Birat, "Renewables-based Decarbonization and Relocation of Iron and Steel Making A Case Study", doi: 10.1111/jiec.12997.

Grigoriev, S.A., Fateev, V.N., Bessarabov, D.G., Millet, P., 2020. Current status, research trends, and challenges in water electrolysis science and technology. Int. J. Hydrogen Energy 45 (49), 26036–26058. https://doi.org/10.1016/J.IJHYDENE.2020.03.109. Oct.

Hosseinzadeh, M., Mashhadimoslem, H., Maleki, F., Elkamel, A., 2022. Prediction of solid conversion process in direct reduction iron oxide using machine learning. Energies 15 (24). https://doi.org/10.3390/en15249276. Dec.

Hou, B., Zhang, H., Li, H., Zhu, Q., 2012. Study on kinetics of iron oxide reduction by hydrogen. Chin. J. Chem. Eng. 20 (1), 10–17. https://doi.org/10.1016/S1004-9541(12)60357-7. Feb.

Hoxha, J.-L., et al., 2020. Feasibility study of low-carbon ammonia and steel production in Europe [Online]. https://web.fe.up.pt/~fgm/eurecha/scp_2019/2ndPrize_Report_Eurecha_SCP2019_ULiege.pdf. (Accessed 26 May 2023).

Islam, K.M.N., 2018. Municipal solid waste to energy generation: an approach for enhancing climate co-benefits in the urban areas of Bangladesh. Renew. Sustain. Energy Rev. 81, 2472–2486. https://doi.org/10.1016/J.RSER.2017.06.053. Jan.

ISPRA, "Indicatori di efficienza e decarbonizzazione del sistema energetico nazionale e del settore elettrico." Accessed: Mar. 09, 2023. [Online]. Available: https://www.isprambiente.gov.it/files2022/pubblicazioni/rapporti/r363-2022.pdf.

Jensen, C., Duyar, M.S., 2021. Thermodynamic analysis of dry reforming of methane for valorization of landfill gas and natural gas. Energy Technol. 9 (7) https://doi.org/10.1002/ENTE.202100106. Jul.

Jiang, X., Wang, L., Shen, F.M., 2013. Shaft furnace direct reduction technology - midrex and Energiron. Adv. Mater. Res. 805–806, 654–659. https://doi.org/10.4028/WWW.SCIENTIFIC.NET/AMR.805-806.654.

Khallaghi, N., Hanak, D.P., Manovic, V., 2020. Techno-economic evaluation of near-zero CO2 emission gas-fired power generation technologies: a review. J. Nat. Gas Sci. Eng. 74, 103095 https://doi.org/10.1016/J.JNGSE.2019.103095. Feb.

M. Kirschen et al., "Off-gas measurements for mass and energy balances of stainless steel EAF. Increasing lifetime of metallic recirculating radiant tubes View project Numerical modelling of the vacuum arc remelting process View project OFF-GAS MEASUREMENTS FOR MASS AND ENERGY BALANCES OF A STAINLESS STEEL EAF," 2001. [Online]. Available: https://www.researchgate.net/publication/276409331.

Kirschen, M., Badr, K., Pfeifer, H., 2011. Influence of Direct Reduced Iron on the Energy Balance of the Electric Arc Furnace in Steel Industry. https://doi.org/10.1016/j.energy.2011.07.050.

Kirschen, M., Badr, K., Pfeifer, H., 2011. Influence of direct reduced iron on the energy balance of the electric arc furnace in steel industry. Energy 36 (10), 6146–6155. https://doi.org/10.1016/J.ENERGY.2011.07.050. Oct.

Kirschen, M., Hay, T., Echterhof, T., 2021. Process improvements for direct reduced iron melting in the electric arc furnace with emphasis on slag operation. Processes 9 (2), 1–10. https://doi.org/10.3390/pr9020402. Feb.

Krüger, A., Andersson, J., Grönkvist, S., Cornell, A., 2020. Integration of water electrolysis for fossil-free steel production. Int. J. Hydrogen Energy 45 (55), 29966–29977. https://doi.org/10.1016/J.IJHYDENE.2020.08.116. Nov.

Lee, H., Lee, J., Koo, Y., 2022. Economic impacts of carbon capture and storage on the steel industry–A hybrid energy system model incorporating technological change. Appl. Energy 317. https://doi.org/10.1016/J.APENERGY.2022.119208, 119208, Jul.

Longbottom, R.J., Kolbeinsen, L., Longbottom, R., 2008. Iron Ore Reduction with CO and H2 Gas Mixtures-Thermodynamic and Kinetic Modelling. Feb. 27, 2023. [Online]. Available: https://ro.uow.edu.au/engpapers/1260.

Lopez, G., Farfan, J., Breyer, C., 2022. Trends in the global steel industry: evolutionary projections and defossilisation pathways through power-to-steel. J. Clean. Prod. 375, 134182 https://doi.org/10.1016/J.JCLEPRO.2022.134182.

Mandova, H., Gale, W.F., Williams, A., Heyes, A.L., Hodgson, P., Miah, K.H., 2018. Global Assessment of Biomass Suitability for Ironmaking-Opportunities for Co-location of Sustainable Biomass, Iron and Steel Production and Supportive Policies. https://doi.org/10.1016/j.seta.2018.03.001.

Manocha, S., Ponchon, F., 2018. Management of lime in steel. Metals 8 (9). https://doi.org/10.3390/met8090686. MDPI AG, Sep. 01.

Midrex, "The MIDREX® Process - Optimizing DRI production using natural gas." Accessed: Mar. 06, 2023. [Online]. Available: https://www.midrex.com/wp-content/uploads/MIdrex_Process_Brochure_4-12-18.pdf.

Midrex, "The MIDREX® Process-The world's most reliable and productive Direct Reduction Technology", Accessed: Mar. 06, 2023. [Online]. Available: https://www.midrex.com/wp-content/uploads/MIdrex_Process_Brochure_4-12-18.pdf.

R. Millner et al., "MIDREX H2-The Road to CO2-free Direct Reduction", Accessed: Mar. 21, 2023. [Online]. Available: https://www.primetals.com/fileadmin/user_upload/landing_pages/2021/Green_Steel/Publications/downloads/AISTech_2021_MIDREX_H2_Final.pdf.

Mondal, K., Lorethova, H., Hippo, E., Wiltowski, T., Lalvani, S.B., 2004. Reduction of iron oxide in carbon monoxide atmosphere - reaction controlled kinetics. Fuel Process. Technol. 86 (1), 33–47. https://doi.org/10.1016/j.fuproc.2003.12.009. Nov.

Nasiri, Y., Panjepour, M., Ahmadian, M., 2016. The kinetics of hematite reduction and cementite formation with CH4-H2-Ar gas mixture. Int. J. Miner. Process. 153, 17–28. https://doi.org/10.1016/j.minpro.2016.05.017. Aug.

Nayional Petroleum Council, 2019. Meeting the Dual Challenge A Roadmap to At-Scale Deployment of Carbon Capture, Use, and Storage. Appendix E: Mature CO2 Capture Technologies. Mar. 24, 2023. [Online]. https://www.energy.gov/sites/default/files/2021-06/2019%20-%20Meeting%20the%20Dual%20Challenge%20Vol%20III%20Appendix%20E.pdf.

Nduagu, E.I., et al., 2022. Comparative life cycle assessment of natural gas and coal-based directly reduced iron (DRI) production: a case study for India. J. Clean. Prod. 347 https://doi.org/10.1016/j.jclepro.2022.131196.

Neuwirth, M., Fleiter, T., Manz, P., Hofmann, R., 2021. The Future Potential Hydrogen Demand in Energy-Intensive Industries-A Site-specific Approach Applied to Germany. https://doi.org/10.1016/j.enconman.2021.115052.

Nurdiawati, A., Zaini, I.N., Wei, W., Gyllenram, R., Yang, W., Samuelsson, P., 2023. Towards fossil-free steel: life cycle assessment of biosyngas-based direct reduced iron (DRI) production process. J. Clean. Prod. 393, 136262 https://doi.org/10.1016/J.JCLEPRO.2023.136262.

Olayebi, O.O., 2014. The midrex process and the Nigerian steel industry. Int. J. Eng. Sci. 3 (11) [Online]. http://www.ijesrt.com.

Pardo, N., Moya, J.A., 2013. Prospective scenarios on energy efficiency and CO2 emissions in the European Iron & Steel industry. Energy 54, 113–128. https://doi.org/10.1016/j.energy.2013.03.015. Jun.

Parisi, D.R., Laborde, M.A., 2004. Modeling of counter current moving bed gas-solid reactor used in direct reduction of iron ore. Chem. Eng. J. 104 (1–3), 35–43. https://doi.org/10.1016/J.CEJ.2004.08.001. Nov.

Patisson, F., Mirgaux, O., Birat, J.P., 2021. Hydrogen steelmaking. Part 1: physical chemistry and process metallurgy. Matériaux Tech. 109 (3–4), 303. https://doi.org/10.1051/MATTECH/2021025.

Ranzani Da Costa, A., Wagner, D., Patisson, F., 2013. Modelling a new, low CO2 emissions, hydrogen steelmaking process. J. Clean. Prod. 46, 27–35. https://doi.org/10.1016/J.JCLEPRO.2012.07.045.

Remus, Rainer, Roudier, Serge, Aguado-Monsonet, M.A., 2013. Luis. Delgado sancho, and institute for prospective technological studies. Best Available Techniques (BAT) Reference Document:for:Iron and Steel Production:Industrial Emissions Directive 2010/75/EU:(Integrated Pollution Prevention and Control) 597. https://doi.org/10.2791/98516.

Rispoli, A.L., et al., 2021. Simultaneous decarbonisation of steel and Oil&Gas industry by MSW gasification: economic and environmental analysis. Energy Convers. Manag. 245 https://doi.org/10.1016/J.ENCONMAN.2021.114577. Oct.

Rochelle, G.T., 2014. Postcombustion Capture Amine Scrubbing.

Rosner, F., et al., 2023. Green steel: design and cost analysis of hydrogen-based direct iron reduction. Energy Environ. Sci. https://doi.org/10.1039/D3EE01077E.

Salman, C.A., Omer, C.B., 2020. Process modelling and simulation of waste gasification-based flexible polygeneration facilities for power, heat and biofuels production. Energies 13 (6). https://doi.org/10.3390/en13164264. Aug.

T. K. Sandeep Kumar, H. Ahmed, J. Alatalo, and B. Björkman, "Carburization behavior of hydrogen-reduced DRI using synthetic bio-syngas mixtures as fossil-free carbon sources," J. Sustain. Metallurgy, vol. 8, pp. 1546–1560, 1234, doi: 10.1007/s40831-022-00590-0.

Santos, S., 2014. CO2 capture in the steel industry. Review of the current state of art [Online]. https://ieaghg.org/docs/General_Docs/IEAGHG_Presentations/SSantos_IEAGHG_-_Iron_Steel_CCSSEC.pdf. (Accessed 26 May 2023).
S. Sarkar, R. Bhattacharya, G. Gopal Roy, and P. Kumar Sen A, "Modeling MIDREX Based Process Configurations for Energy and Emission Analysis", doi: 10.1002/srin.201700248.
Shams, A., Moazeni, F., 2015. Modeling and simulation of the MIDREX shaft furnace: reduction, transition and cooling zones. JOM (J. Occup. Med.) 67 (11), 2681–2689. https://doi.org/10.1007/s11837-015-1588-0. Aug.
J. Sloop, "Direct from MIDREX workplace safety-a matter of dollars and sense." Accessed: May 26, 2023. [Online]. Available: https://www.midrex.com/commentary/workplace-safety-a-matter-of-dollars-and-sense/.
Smith Lewin, C., Fonseca de Aguiar Martins, A.R., Pradelle, F., 2020. Modelling, simulation and optimization of a solid residues downdraft gasifier: application to the co-gasification of municipal solid waste and sugarcane bagasse. Energy 210. https://doi.org/10.1016/j.energy.2020.118498. Nov.
Stanley, Santos, 2013. Iron and Steel CCS Study (Techno-Economics Integrated Steel Mill), vol. 1. IEAGHG, Cheltenham.
Strezov, V., Evans, A., Evans, T., 2013. Defining sustainability indicators of iron and steel production. J. Clean. Prod. 51, 66–70. https://doi.org/10.1016/J.JCLEPRO.2013.01.016.
Suer, J., Traverso, M., Jäger, N., 2022. Review of life cycle assessments for steel and environmental analysis of future steel production scenarios. Sustainability 14 (21). https://doi.org/10.3390/su142114131. MDPI, Nov. 01.
Trinca, A., Bassano, C., Verdone, N., Deiana, P., Vilardi, G., 2023. Modelling and economic evaluation of CCS/PtX technologies integrated into biomass MTG plants. J. Environ. Chem. Eng. 11 (1) https://doi.org/10.1016/j.jece.2022.109184.
R. Turton, Bailie RC, Whiting WB, Shaeiwitz JA, and Bhattacharyya D, Analysis, Synthesis, and Design of Chemical Processes, fourth ed..
Vogl, V., Åhman, M., Nilsson, L.J., 2018. Assessment of hydrogen direct reduction for fossil-free steelmaking. J. Clean. Prod. 203, 736–745. https://doi.org/10.1016/J.JCLEPRO.2018.08.279. Dec.
Xiao, M., Junne, T., Haas, J., Klein, M., 2021. Plummeting costs of renewables - are energy scenarios lagging? Energy Strategy Rev. 35, 100636 https://doi.org/10.1016/J.ESR.2021.100636. May.
Ye, G., Xie, D., Qiao, W., Grace, J.R., Lim, C.J., 2009. Modeling of fluidized bed membrane reactors for hydrogen production from steam methane reforming with Aspen Plus. Int. J. Hydrogen Energy 34 (11), 4755–4762. https://doi.org/10.1016/J.IJHYDENE.2009.03.047.
Yilmaz, C., Wendelstorf, J., Turek, T., 2017. Modeling and Simulation of Hydrogen Injection into a Blast Furnace to Reduce Carbon Dioxide Emissions. https://doi.org/10.1016/j.jclepro.2017.03.162.
Carbon Capture Carbon Capture & Use - Midrex Technologies, Inc. https://www.midrex.com/carbon-capture-use/(accessed May 22, 2023).
"EU Natural Gas - 2023 Data - 2010-2022 Historical - 2024 Forecast - Price - Quote." https://tradingeconomics.com/commodity/eu-natural-gas (accessed Mar. 28, 2023).
How Much Does Limestone Cost? | HowMuchIsIt.org. https://www.howmuchisit.org/how-much-does-limestone-cost/(accessed, Mar. 28, 2023.
"Coal PRICE Today | Coal Spot Price Chart | Live Price of Coal per Ounce | Markets Insider." https://markets.businessinsider.com/commodities/coal-price (accessed Mar. 28, 2023).
"Getting the Most From Direct Reduced Iron - Operational Results of MIDREX® Hot Transport-Hot Charging - Midrex Technologies, Inc." https://www.midrex.com/tech-article/getting-the-most-from-direct-reduced-iron-operational-results-of-midrex-hot-transport-hot-charging/(accessed May 16, 2023).
"IEA G20 Hydrogen Report: Assumptions".
"Electricity prices in Europe fell in January 2023 – Energy Crisis." https://gmk.center/en/posts/electricity-prices-in-europe-fell-significantly-in-january-2023/(accessed Mar. 28, 2023).
"Demand in the iron ore DR pellet market improves on lower premium - Fastmarkets." https://www.fastmarkets.com/insights/demand-iron-ore-dr-pellet-market-improves (accessed August 23, 2023).
"Electric Power Monthly - U.S. Energy Information Administration (EIA)." https://www.eia.gov/electricity/monthly/epm_table_grapher.php?t=epmt_5_6_a (accessed May 23, 2023).
"Qual è lo stipendio medio delle diverse professioni?" https://www.kellyservices.it/stipendio-medio (accessed Mar. 30, 2023).
"Price History Tables and Charts USA China Western Europe World Export", Accessed: Mar. 28, 2023. [Online]. Available: www.steelbenchmarker.com.
sono l'energia del futuro o la speculazione del secolo? - ilSole24ORE. https://www.econopoly.ilsole24ore.com/2022/01/19/rinnovabili-energia-speculazione/(accessed, Maro. 28, 2023.
"Italy Electricity Price - 2023 Data - 2004-2022 Historical - 2024 Forecast - Quote." https://tradingeconomics.com/italy/electricity-price (accessed Jun. 30, 2023).
Impact of Hydrogen DRI on EAF Steelmaking - Midrex Technologies, Inc. https://www.midrex.com/tech-article/impact-of-hydrogen-dri-on-eaf-steelmaking/(accessed. (Accessed 27 February 2023).
"Why MOFs outperform amine scrubbing?" https://blog.novomof.com/why-mofs-outperform-amine-scrubbing (accessed Mar. 28, 2023).
"United States Natural Gas Industrial Price (Dollars per Thousand Cubic Feet)." https://www.eia.gov/dnav/ng/hist/n3035us3m.htm (accessed May 23, 2023).
Direct Reduction Plants - 2019 Operations Summary - Midrex Technologies, Inc. https://www.midrex.com/tech-article/midrex-direct-reduction-plants-2019-operations-summary/(accessed. (Accessed 21 March 2023).